IEEE Access
Multidisciplinary | Rapid Review | Open Access Journal

Received March 17, 2022, accepted April 10, 2022, date of publication April 18, 2022, date of current version April 29, 2022.

Digital Object Identifier 10.1109/ACCESS.2022.3168321

Age of Information in CSMA-Based Networks With Bursty Update Traffic

ANDREA BAIOCCHI[1], (Member, IEEE), ION TURCANU[2], (Member, IEEE), AND ALEXEY VINEL[3,4], (Senior Member, IEEE)

[1]Department of Information Engineering, Electronics and Telecommunications (DIET), Sapienza University of Rome, 00184 Rome, Italy
[2]Luxembourg Institute of Science and Technology (LIST), 4362 Esch-sur-Alzette, Luxembourg
[3]School of Information Technology, Halmstad University, 301 18 Halmstad, Sweden
[4]Chair of Reliable Distributed Systems, University of Passau, 49032 Passau, Germany

Corresponding author: Andrea Baiocchi (andrea.baiocchi@uniroma1.it)

This work was supported in part by the Swedish Knowledge Foundation (KKS) for the "Safety of Connected Intelligent Vehicles in Smart Cities—SafeSmart" Project (2019–2023), in part by the Swedish Innovation Agency (VINNOVA) for the "Emergency Vehicle Traffic Light Preemption in Cities—EPIC" Project (2020–2022), and in part by the Excellence Center at Linköping – Lund in Information Technology (ELLIIT) Strategic Research Network.

ABSTRACT Exchanging status information between closely located mobile agents is an underlying process in numerous future Cyber Physical System (CPS). Real-time updates including positions of neighboring nodes is performed when, for example, autonomous vehicles execute a cooperative maneuver, industrial robots collaborate with each other on a task, or Unmanned Aerial Vehicles (UAVs) execute a mission in a swarm. For the design of networked automatic control strategies in these scenarios, it is essential to understand the performance of such Machine-to-Machine (M2M) communications from the information freshness perspective. To this end, we introduce a mathematical framework which allows characterizing the Age of Information (AoI) in networks governed by the Carrier-Sense Multiple Access (CSMA) protocol. Differently from existing work, we take into account the fact that update packets sent by mobile nodes are not necessarily periodic, since packet triggering is often coupled with agents' mobility. Our approach is based on the assumption that diverse mobility-triggered message generation patterns can be modeled by a wide class of update traffic arrival processes. We apply Discrete Markovian Arrival Process (DMAP), which is a versatile arrival model able to fit arrival patterns that are modulated by a finite state machine, including bursty traffic. We develop an accurate and efficient analytical model of nodes exchanging one-hop broadcast update messages with bursty arrivals to evaluate the moments as well as entire probability distribution of several performance metrics, including AoI. An asymptotic analysis for large networks suggests a simple way to control the update message rate to minimize the AoI. We show that the optimal update rate that minimizes the mean AoI coincides with the optimum of the wireless channel utilization. Numerical examples point out that the asymptotic theory provides accurate predictions also for small values of the number of nodes.

INDEX TERMS Age of information, CSMA networks, cyber-physical system, full connectivity, MAC access delay, machine-to-machine communications, V2X networks.

I. INTRODUCTION

Cyber Physical System (CPS) stemming from the Internet of Things (IoT) paradigm rely on monitoring and control processes running on distributed agents interacting by means of update message exchanges which convey locally collected data. Examples of such Machine-to-Machine (M2M) communication environments can be found in Cooperative Intelligent Transport System (C-ITS) with cooperative maneuvering of automated vehicles [1], where real-time updates are crucial for safe driving. Another instance of cooperating agents is provided by swarms of aerial vehicles that move in a coordinated way, e.g., in rescue operations, surveillance, exploration, and many other missions that require tight cooperation among nodes [2]. Other notable examples can be found in industrial processes automation, where teams of robots and moving machines cooperate in assembly lines. Also, logistics is increasingly automated and realized by moving robots in large store plants [3].

In all mentioned examples, the generation of update messages can be either periodic or event-driven. The latter case has received less attention in the literature so far and is

The associate editor coordinating the review of this manuscript and approving it for publication was Ding Xu.

This work is licensed under a Creative Commons Attribution 4.0 License. For more information, see https://creativecommons.org/licenses/by/4.0/

a subject of our study. In this context, the notion of event can be miscellaneous, but most often is coupled to the mobility of agents. For example, if the change of the agent coordinate since the last update exceeds a certain threshold, a new packet will be triggered. This implies that the faster an agent moves, more frequently it generates updates [4]. Such an approach results in a bursty update traffic, which we assume is communicated via one-hop broadcast packets exchange between the agents located in a close proximity.

Communications are supported via radio channels. Current and foreseeable supporting technologies fall into two categories: wireless networking, e.g., the IEEE 802.11 family, and cellular networking, currently dominated by 5G solutions (e.g., see M2M or the Ultra-Reliable Low Latency Communication paradigms). In this work we focus on the Vehicle-to-Everything (V2X) network application case and on Carrier-Sense Multiple Access (CSMA) networks, as used specifically in the Wi-Fi amendment devised for vehicular applications, IEEE 802.11p [5], and its evolution, IEEE 802.11bd [6]. We consider one-hop broadcast message exchange, which is the core functionality of cooperative awareness among vehicle agents. The presented model has however a broader range of applicability, e.g., in the IoT framework, since the core assumptions of the model are that the wireless channel is shared according to non-persistent CSMA and packet traffic consists of one-hop broadcast messages.

The most relevant performance metric in the context of this study is the Age of Information (AoI) [7], a measure of data freshness stored in each node's local data base, updated upon the reception of new messages from neighboring nodes. The AoI requirements on advanced V2X use-cases are becoming more and more stringent. Both IEEE 802.11p and upcoming CSMA/CA based technologies, i.e. IEEE 802.11bd, should be configured properly to support these requirements. As an example, the 5G Automotive Association (5GAA) defines the latency requirements as low as 10 ms (e.g., ''automated intersection crossing'' requires 10 ms latency, ''cooperative lane merge'' requirement is 20 ms [8]). This strict requirement must account for several sources of delay in the process that encompasses data measurement, processing and delivering. In-vehicle networking, interconnecting on-board sensors and communication equipment, is one component of end-to-end delay [9]. Another source of delay comes from security overhead [10]. These delays could put pressure on the actual V2X delay even more. When one sums up all the aforementioned latency sources, it becomes obvious that, in order to fulfill the stringent C-ITS requirements, V2X systems should be accurately configured to meet AoI requirements and avoid additional sources of delays in medium access, packet losses, and collisions.

To this end, we aim at providing the following two main original contributions:

- An analytical model characterizing one-hop broadcast update messages in CSMA networks to evaluate the probability distribution of AoI for nodes with *bursty traffic arrivals* – a distinguishing feature of our proposed solution compared to the state of the art;
- An asymptotic analysis for large CSMA networks that suggests a simple way to control the update message rate to minimize the AoI.

The proposed model is able to predict average values as well as probability distributions with remarkable accuracy. The model is fairly general to deal with correlated arrivals and variable message sizes.

The rest of the paper is organized as follows. Section II presents the relevant literature. Section III introduces the modeling approach and the main assumptions. The proposed model is analyzed in Section IV, where the Probability Density Functions (PDFs) of all main model variables are derived, and expressions of key performance metrics are given, including AoI. In Section V the model is validated against simulations, while in Section VI the asymptotic analysis is provided to derive, in particular, a closed form expressions of the optimized message generate rate and the corresponding AoI. Finally, conclusions are drawn in Section VII, including hints at possible extensions of the model.

II. RELATED WORK

AoI has been first introduced by Kaul *et al.* [11] as a general metric to evaluate the performance of status update systems. The methods introduced in [11] can be applied to a wide class of service systems that can be abstracted as consisting of a source, a service facility, and a monitor. The authors explore a First Come First Served (FCFS) queue discipline, demonstrating that an optimal information generation rate exists. A similar system abstraction is considered in [12], where the authors focus on the stationary distribution of AoI under FCFS and Last Come First Served (LCFS) queue disciplines. The LCFS queue discipline is also considered by Bedewy *et al.* [13], who analyze the AoI in interference-free multi-hop networks. Since we consider a status update system, in this work we assume single-packet queues (i.e., nodes can keep only one message in the queue), since any updates arriving from the application would simply substitute any existing message in the queue.

Many related studies have focused on a specific class of systems in which nodes send periodic updates to a central monitoring station. For example, Kadota *et al.* [14] consider the problem of minimizing the AoI under throughput constraints in a single-hop wireless network in which nodes transmit information to a base station. The authors later extended this work to address the link scheduling optimization problem in networks with stochastic packet arrivals and unreliable links [15]. Scheduling policies for minimizing the AoI in single-hop multi-server queuing systems are also studied in [16]. Liu and Bennis [17] use the Extreme Value Theory (EVT) to characterize the maximal AoI in wireless industrial networks. They formulate an optimization problem to minimize the sensors' transmit power and propose a dynamic policy for resource allocation and status updates. Chen *et al.* [18] study the case when multiple packets form a certain piece of

information. They propose a Whittle index-based scheduling mechanism at the base station to minimize the AoI of such systems with variable information size.

The AoI metric has been used in a number of different application domains. In a recent work, Gómez *et al.* [19] introduce the AoI concept in nanonetworks, in which nanodevices exchange information over molecular communication channels. To analyze the trade-off between the transmission rate and produced inter-symbol interference, the authors focus on the peak AoI, which describes the maximum AoI for each packet. Abd-Elmagid and Dhillon [20] exploit Unmanned Aerial Vehicles (UAVs) to act as mobile relays in order to minimize the mean peak AoI for a source-destination pair. To this end, they formulate an optimization problem that jointly optimizes the UAV's trajectory, as well as energy and service time allocations. Bedewy *et al.* [21] consider a wireless network in which low-power devices send status updates to a common access point. The proposed solution aims at minimizing the peak AoI while meeting energy constraints. Sinha and Roy [22] study the concept of AoI in the context of industrial Time-Division Multiple Access (TDMA)-based wireless networks for cyber physical production systems. The authors propose two greedy scheduling algorithms, analyzing their optimality via extensive simulations. Hirosawa *et al.* [23] propose new resource allocation algorithms to minimize the mean AoI in energy harvesting wireless sensor networks, based on both TDMA and Frequency-Division Multiple Access (FDMA) channels. Their results show that the choice of TDMA versus FDMA depends on available resources, data packet size, and time of packet observation in the system. Wei and Deng [24] define a mathematical framework to analyze the peak AoI in large-scale wireless networks using rateless codes. The authors model the spatial distribution of the information sources as Poisson point process, while the traffic arrival as as an independent Bernoulli process.

AoI has also been studied in CSMA-based communication systems [25]–[29]. In one of our previous works [25], we propose an analytical model that characterizes the AoI of a one-hop CSMA broadcast network with partial sensing. We introduce a simple $M/D/\infty$ queuing model to account for the effect of partial sensing. We demonstrate that the model is able to capture the trade-off between channel load, AoI, and fairness among nodes. Wang and Dong [27] consider a slotted one-hop broadcast CSMA wireless network and propose a model that characterizes the AoI from a transmitter perspective. Maatouk *et al.* [26] tackle the problem of finding the optimal back-off time for links in a CSMA network in order to minimize the mean AoI. They propose closed-form expressions for the average AoI of the network when packets are generated at will or according to a stochastic process. Moltafet *et al.* [28] analyze the average AoI and peak AoI in simplified CSMA-based wireless sensor networks under FCFS policy, by considering a tagged node with Poisson arrivals and all other nodes having saturated queues. Their results indicate that the AoI can be improved by optimizing the contention window size and packet arrival rate. Zhou and Saad [29] also assume Poisson arrivals in a CSMA-based IoT monitoring system composed of pairs of IoT devices, i.e., each sender is associated with a corresponding receiver. The authors derive closed-form expressions for the average AoI of each device and analyze the asymptotic performance of the system for an infinite number of devices.

Several studies analyze the AoI in the context of vehicular networking and C-ITS [30]–[34]. Kaul *et al.* [30] were among the first to propose adaptive beaconing strategies for vehicular networks in order to minimize the AoI. Their proposed solution aims at balancing the load on the wireless network and the update sending frequency. In one of our previous works [33], we compare the performance of the algorithm proposed in [30] with the current Decentralized Congestion Control (DCC) algorithms standardized by the European Telecommunications Standards Institute (ETSI), as well as with a centralized scheduling mechanism that provides a bound on the performance in terms of AoI and congestion level. In [33] we also analyze the trade-off between AoI, reliability, and channel utilization efficiency. In [34], we focus on a vehicular platooning use case and propose a DCC state-machine and gatekeeper configuration to meet the requirements in terms of AoI. The platooning use case has also been considered in [32], where the authors suggest to exploit the number of interfering vehicles to generate AoI samples that can be used by cooperative driving applications. In another study [31], we model the AoI in IEEE 802.11p networks from a single node's perspective, but also from a network point of view. We demonstrate that both models are accurate when evaluating the AoI, but also a number of other relevant metrics.

The model proposed in this paper fits to an IoT environment, where a number of devices exchange update messages with their neighbors, using a CSMA network. Differently from most works, that refer to paradigms with multiple devices uploading their update messages to a sink node or pairs of sender-receiver nodes, we consider multiple sources and multiple sinks. Namely, every node belonging to the network originates update messages, directed to its neighbors. In turn, every node receives update message from each of its neighbors. This is the basic functionality used to build so called cooperative awareness, i.e., to support those functions that require cooperation of distributed agents, which coordinate their efforts. Typical examples of such paradigm are connected vehicles, industrial IoT, UAV swarms.

A major use case of the model presented in this paper is vehicular networking based on IEEE 802.11p/bd technology. The versatile model developed in the paper lends itself to capturing burstiness of update message generation process. To the best of our knowledge, this is a novel feature with respect to the existing studies of one-hop broadcast messaging for cooperative awareness. Our assumption is based on previous experimental studies which have shown that the generation process of update messages, e.g., in the vehicular environment, is not simply periodic [35].

III. SYSTEM MODEL

This section includes (i) notation and general definitions used in the paper, (ii) main model assumptions, and (iii) definition of the node traffic model, i.e., packet transmission times and packet arrival process.

A. NOTATION

We denote random variables with capital letters. Given a discrete-valued random variable X, we denote its Cumulative Distribution Function (CDF), Complementary Cumulative Distribution Function (CCDF) and Probability Distribution Function (PDF) respectively with $F_X(k) = \mathcal{P}(X \leq k)$, $G_X(k) = 1 - F_X(k)$, and $f_X(k) = \mathcal{P}(X = k)$. The symbol $\mathrm{E}[g(X)]$ defines expectation, namely $\mathrm{E}[g(X)] = \sum_k g(k) f_X(k)$, where the summation extends over the entire domain of the random variable X. Analogous definitions and notation hold for continuous-valued random variables.

Generating Functions (GFs) of positive discrete random variables are used. Given a random variable X, with PDF $f_X(k)$, $k \geq 1$, we define the GF of X as $\phi_X(z) = \mathrm{E}[z^X] = \sum_{k \geq 1} z^k f_X(k)$. The GF $\phi_X(z)$ is analytic (at least) for $|z| \leq 1$ and $\phi_X(1) = 1$. We remind that the moments of X can be obtained by deriving the GF. In particular, the first two moments of X are derived as follows: $\mathrm{E}[X] = \phi'_X(1)$ and $\mathrm{E}[X^2] = \phi''_X(1) + \phi'_X(1)$. The variance of X is denoted with σ_X^2. Analogous definitions hold for the Laplace transform of the PDF of continuous-valued positive random variables. Namely, given a positive continuous random variable X with PDF $f_X(t)$, its Laplace transform is denoted with $\varphi_X(s) = \mathrm{E}[e^{-sX}]$. Moments are found here by deriving the Laplace transform and setting $s = 0$, e.g., $\mathrm{E}[X] = -\varphi'_X(0)$ and $\mathrm{E}[X^2] = \varphi''_X(0)$.

Time is measured in units of back-off slot time δ. To highlight normalization, we denote normalized time variables with a hat. As a matter of example, if X denotes a time variable, it is $\hat{X} = X/\delta$.

Table 1 lists the main symbols used in the model and their respective definitions.

B. ASSUMPTIONS

We consider n nodes sharing a wireless channel according to non-persistent CSMA [36]. We sketch concisely the main steps of non-persistent CSMA protocol in the following. The node Medium Access Control (MAC) entity alternates between an idle state, when no packet is to be transmitted, and a backlogged state, when it has a packet ready to be transmitted. A backlogged node senses the channel to assess whether it is busy (another node already transmitting) or idle. Sensing consists of measuring the energy on the channel and comparing it to a threshold. It requires a time depending on the physical layer technology (e.g., for WiFi it is in the order of 10 µs). The time it takes a node to carry out sensing is usually referred to as back-off slot time. A node sensing a busy channel waits for the channel to get back to idle. According to non-persistent approach, as soon as the channel is sensed idle, the node sets a counter to a randomly drawn integer K and starts counting down, i.e., the node decrements the counter by one for each sensed idle back-off slot (i.e., a back-off slot time during which no node transmits on the channel). As the counter eventually hits 0, the node starts transmitting. If the channel is found busy during the countdown process, the node freezes its counter until the channel becomes idle again. At that point the countdown is resumed.

It is assumed that nodes are within each other's range, i.e., there are no hidden nodes. The time axis is divided into *virtual time slots* – i.e., time intervals elapsing between two successive idle back-off time slots. Since there are no hidden nodes, all nodes are ''synchronized'' on virtual time slot boundaries.

The probability of packet reception failure due to the physical layer issues is denoted with Packet Error Ratio (PER). This parameter summarizes the effect of physical channel impairments, taking into account that a packet can be decoded with errors and hence discarded even if it does not incur in a collision. This parameter is meant to be the worst case probability of reception failure. Physical layer mechanisms are assumed to be configured so that the probability that packet decoding fails be no more than PER. The ensuing analysis is therefore conservative under this respect. Note that ACKs and re-transmissions are not envisaged, since we consider broadcast update packets exchanged among nodes.

We refer to a symmetrical scenario, where the statistical characteristics of the traffic offered by the nodes (statistics of arrivals and transmission times) are the same for all the nodes. The proposed model lends itself to being generalized to heterogeneous settings, albeit at the cost of increased complexity. We prefer leaving this issue for future work and focusing on insight gained from the model in its simpler symmetric form in this work.

The model is obtained by considering the point of view of one node, which we refer to as the tagged node for ease of presentation of the model. We drop the subscript denoting the tagged node, unless required to avoid ambiguity. If not stated explicitly, it is understood that any variable or quantity refers to the tagged node. The impact of all other nodes is summarized by means of their probability of transmitting in a virtual time slot. This modeling approach falls into the ''mean field'' approximation realm. It turns out that, in spite of the strong simplification it brings about (the state space of the model is reduced from being an n-dimensional random variable to scalar random variables), it provides highly accurate results. This is consistent with the fact that the mean field approach was proved accurate for the analysis of CSMA in case of saturated traffic regime [37].

C. NODE TRAFFIC MODEL

The traffic model considered in this work is consistent with message flows exchanged by nodes that run distributed cooperative awareness applications that require a steady flow of update messages. Therefore we consider one-hop broadcast packets, i.e., each node sends update messages in broadcast

TABLE 1. Main notation symbols and their definitions.

Symbol	Definition
n	Number of nodes.
λ	Mean arrival rate of new messages at a node.
S	Message generation time. It is $S = 1/\lambda$.
δ	Back-off slot time.
T_{oh}	Overhead time in one packet transmission.
U	Packet payload transmission time.
T	Packet transmission time, $T = T_{\text{oh}} + U$.
b_j	j-th value of the normalized transmission time $\hat{T}$, $j = 1, \ldots, \ell$. It is assumed that $b_1 < b_2 < \cdots < b_\ell$.
W_0	Contention window size.
τ	Transmission probability of one node in a virtual slot time.
q	Probability that nodes other than the tagged one do not transmit in one virtual slot time.
X	Virtual slot time.
C	Service time, i.e., time elapsing since the beginning of countdown until packet transmission completion.
R	Node idle time, i.e., time elapsing since end of transmission of a packet until the beginning of countdown of next packet.
Y	Packet inter-departure time of a node.
N	Number of virtual slot times in an idle time R.
K	Number of virtual slot times counted down in a service time (including the one where transmission occurs).
$A(t)$	Number of arrivals at a node in back-off slot t. It can be either 0 or 1.
$J(t)$	State of the modulating Markov chain of arrival process at a node in back-off slot t. It can take an integer value between 1 and r.
r	Number of states of the modulating Markov chain $J(t)$ of arrival process at a node.
$\mathbf{A}_0$	$r \times r$ matrix whose entry (i, j) is the probability of no arrival ($A(t) = 0$) and transition of $J(t)$ from i to j in one back-off slot.
$\mathbf{A}_1$	$r \times r$ matrix whose entry (i, j) is the probability of one arrival ($A(t) = 1$) and transition of $J(t)$ from i to j in one back-off slot.
$\mathbf{A}$	One-step transition probability matrix of the Markov chain $J(t)$. It is $\mathbf{A} = \mathbf{A}_0 + \mathbf{A}_1$.
$\mathbf{e}$	r-dimensional column vector of ones.
$\mathbf{I}$	$r \times r$ identity matrix.
$\mathbf{w}$	r-dimensional row vector containing the probability distribution of $J(t)$ sampled upon packet transmission ends.
PER	Packet error ratio, i.e., probability that a packet is decoded with errors due to physical channel impairments.
γ	Probability of successful reception of a packet.
ρ	Channel busy ratio, i.e., mean fraction of time that channel is sensed busy by a tagged node (including transmission time of node itself).
θ	Throughput of a node, i.e., ratio of mean message delivery rate to mean message generation rate.
ψ	Channel utilization coefficient, i.e., mean fraction of channel time used successfully.
D	Access delay, i.e., time elapsing since packet arrival until end of its transmission.
H	AoI of updates received from other nodes.
H_{P}	Peak AoI, maximum age achieved by data stored at a node immediately before receiving an update.

to all its neighbors. A typical use case of this traffic pattern is found in vehicular networking, e.g., with Cooperative Awareness Messages (CAMs). Since only broadcast traffic is used, no ACK is envisaged, hence no re-transmission mechanism is in place.

1) PACKET HANDLING AT NODE MAC LEVEL

Since we refer to update message traffic, where freshness of information is the key requirement, it turns out that buffering more than a single packet is deleterious [38]. Therefore, we assume that at most one packet can be standing in the node MAC entity. Newly arriving messages could overwrite the packet standing in the MAC entity, waiting to be transmitted (preemptive LCFS). In practice, decoupling between the application level, where messages are generated, and MAC level, where messages are handled to be transmitted over the channel, makes preemptive LCFS not easy to implement. Further, preemptive LCFS can only improve the access delay component of the AoI metric. Numerical results suggest that this is often a relatively small part of the overall value of AoI, thus making the more complicate preemptive LCFS not so valuable for reducing AoI Moreover, message inter-arrival times are often much bigger than the time it takes the MAC entity to carry out contention and transmit the message. So, preemptive LCFS entails marginal differences[1] with respect to simpler FCFS with a queue limited to at most one packet. The proposed model can be applied to either strategy, the only key assumption being that at most one packet can be standing in the MAC entity at any given time and no further buffering is provided. In the following we assume a simple non-preemptive policy at the one-packet node buffer.

2) PACKET TRANSMISSION TIMES

Let T_{oh} be the fixed duration of overhead, i.e., preamble, header and trailer, Arbitration Inter-Frame Spacing (AIFS). The transmission time can be modeled as a random variable T given by $T = T_{\text{oh}} + U$, where U is the time required to transmit the payload. It depends on the payload length and selected air bit rate. In the following, it is assumed that T is an integer multiple of the back-off slot time δ, i.e., $\hat{T} = T/\delta$ is an integer-valued random variable. While allowing discrete time models and some formal simplification, this assumption has a negligible impact on accuracy, given the large mismatch of numerical values between the back-off slot time (in the order of several µs) and transmission time (typically ranging between hundreds of µs to few ms). In general, $\hat{T}$ is a discrete

[1]Except when the load offered to the network drives the channel to saturation.

random variable that can take a finite spectrum of values $\{b_1, \ldots, b_\ell\}$, where $b_1 < b_2 < \cdots < b_\ell$, and ℓ is the number of different values of normalized transmission time.

3) PACKET ARRIVAL PROCESS

Arrivals occur according to a Discrete Markovian Arrival Process (DMAP), with time-step size equal to the back-off slot time. DMAP is a Markov modulated arrival process, where the probability of seeing an arrival in a slot is dependent on the state of an underlying modulating finite Markov chain.

DMAP is a versatile arrival model, that encompasses most well-known arrival processes, including renewal type arrivals, ON-OFF arrivals, phase-type arrivals [39]. It offers a modeling option often amenable to mathematical analysis. It is a rich enough model to fit a large variety of arrival patterns found in applications. Random arrivals whose mean rate is a function of a finite state machine can be naturally captured by the DMAP framework, by defining a modulating Markov chain that models the finite state machine and assigning suitable probability of arrivals in each state of the modulating process. We provide examples of DMAP instances representing ON-OFF traffic sources with numerical example in later sections.

Formally, DMAP is defined as a bi-dimensional random process $(A(t), J(t))$, where t is the discrete time index. $A(t)$ is a binary random variable, equal to 1, if there is an arrival in slot t, and 0 otherwise. $J(t)$ is a finite, irreducible Markov chain on the state space $\{1, \ldots, r\}$, r being a positive integer that gives the modulating Markov chain size. The probability that $A(t)$ is 1 depends on the modulating Markov chain state $J(t)$, which is often referred to as the *phase* of the DMAP process.

DMAP is parametrized by two matrices: $\mathbf{A}_0$ and $\mathbf{A}_1$. Their entries have the following meaning. The (i, j) entry $a_{0,ij}$ of $\mathbf{A}_0$ is the probability that $J(t)$ makes a transition from i to j and no arrival occurs, i.e., we let for $i, j = 1, \ldots, r$:

$$a_{0,ij} = \mathcal{P}(A(t+1) = 0, J(t+1) = j \,|\, J(t) = i) \tag{1}$$

Analogously, the (i, j) entry $a_{1,ij}$ of $\mathbf{A}_1$ is the probability that $J(t)$ makes a transition from i to j and there is one arrival, i.e., we let for $i, j = 1, \ldots, r$:

$$a_{1,ij} = \mathcal{P}(A(t+1) = 1, J(t+1) = j \,|\, J(t) = i) \tag{2}$$

Note that $\mathbf{A} = \mathbf{A}_0 + \mathbf{A}_1$ is the one-step transition probability matrix of the Markov chain $J(t)$. It is therefore an $r \times r$ stochastic matrix. We assume further that $\mathbf{A}$ is irreducible. The matrices $\mathbf{A}_0$ and $\mathbf{A}_1$ are sub-stochastic.

The following notation is introduced as well. Let $\mathbf{I}$ be the $r \times r$ identity matrix and $\mathbf{e}$ a column vector of 1's of size r. The mean arrival rate of DMAP is denoted by $\hat{\lambda}$. It is $\hat{\lambda} = \pi \mathbf{A}_1 \mathbf{e}$, where π is the steady-state PDF of the Markov chain $J(t)$, i.e., $\pi_j = \mathcal{P}(J(t) = j)$, $j = 1, \ldots, r$. The PDF π is found by solving the linear equation system $\pi = \pi \mathbf{A}$ with the normalization constraint $\pi \mathbf{e} = 1$. Note that $1/\hat{\lambda}$ is the mean number of back-slots between two consecutive arrivals.

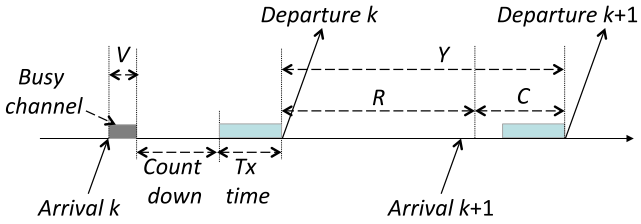

FIGURE 1. Time evolution of the channel as seen by the tagged node and definition of main time intervals of the model.

IV. MODEL ANALYSIS

Sections IV-A to IV-C introduce the main model variables and derive the transforms of their respective probability distributions along with the first two moments. Section IV-D is devoted to the derivation of expressions for all main performance metrics, including access delay and AoI. These four subsections analyze the model in case of fixed transmission times, which leads to more insightful mathematical expressions. This restriction is relaxed in Section IV-E, which is devoted to generalizing the model to the case of variable packet transmission times.

A. VIRTUAL SLOT TIME AND SERVICE TIME

The time axis evolution as seen by the tagged node is sketched in Figure 1. The main model variables are highlighted in the figure and are formally defined in the following.

The probability that no other node transmits when the tagged node is not transmitting is expressed as

$$q = (1 - \tau)^{n-1} \tag{3}$$

where n is the number of nodes (including the tagged one) and τ is the probability that a node transmits in a virtual slot time. We will see later on that τ is computed by means of a fixed point equation.

Let $T = b_1 \delta$ be the fixed transmission time, where b_1 is an integer. The virtual time slot duration as seen by the tagged node is denoted with $\hat{X}$. This is the duration of the virtual slot time when the tagged node is not transmitting. A virtual slot consists of a single back-off slot of duration δ, if no node transmits. On the contrary, if at least one node (other than the tagged one) starts a transmission after sensing an idle back-off slot time, the virtual slot lasts $\delta + T$. Then

$$\hat{X} = \begin{cases} 1 & \text{with probability } q \\ 1 + b_1 & \text{with probability } 1 - q. \end{cases} \tag{4}$$

The GF of the PDF of $\hat{X}$ is

$$\phi_{\hat{X}}(z) = qz + (1 - q) z^{b_1 + 1} \tag{5}$$

Let $\hat{C}$ denote the packet service time, defined as the time elapsing from the beginning of countdown after the arrival of a new packet, until the packet transmission is completed (including the ensuing AIFS required for any other action on the wireless channel to be taken by any node).

The tagged node decrements its back-off counter by one for each idle back-off slot time it sees on the channel. If we

denote the initial counter level with K, the service time C consists of $K-1$ virtual slot times and a final transmission time, where the tagged node transmits, possibly along with other nodes (collision). Therefore, we have

$$\hat{C} = \sum_{j=1}^{K-1} \hat{X}(j) + 1 + b_1 \tag{6}$$

where K is a discrete random variable with uniform probability distribution over the set $\{1, \ldots, W_0\}$, W_0 being a positive integer that represents the contention window size.

The GF of the PDF of $\hat{C}$ is (see Equation (6))

$$\phi_{\hat{C}}(z) = z^{b_1+1} \frac{1 - \phi_{\hat{X}}(z)^{W_0}}{W_0[1 - \phi_{\hat{X}}(z)]}. \tag{7}$$

The first two moments of $\hat{C}$ can be found by deriving the GF of the PDF of $\hat{C}$ and setting $z = 1$ in the derivatives, or directly from the definition of $\hat{C}$ in Equation (6) as the sum of independent random variables. The result is:

$$\mathrm{E}[\hat{C}] = 1 + b_1 + \frac{W_0 - 1}{2} \mathrm{E}[\hat{X}] \tag{8}$$

$$\sigma^2_{\hat{C}} = \frac{W_0^2 - 1}{12} (\mathrm{E}[\hat{X}])^2 + \frac{W_0 - 1}{2} \sigma^2_{\hat{X}} \tag{9}$$

B. IDLE AND INTER-DEPARTURE TIMES

The time $\hat{R}$ from a packet departure until the beginning of the service time of the next arriving packet is the sum of N consecutive virtual time slots:

$$\hat{R} = \sum_{j=1}^{N} \hat{X}(j) \tag{10}$$

where N is a discrete random variable, defined as the number of virtual slots since the end of transmission of a packet until the beginning of countdown of the next arriving packet.

The GF of the idle time R is derived in Appendix. The final result is

$$\phi_{\hat{R}}(z) = \mathbf{w} \left[\mathbf{I} - \phi_{\hat{X}}(\mathbf{A}_0 z)\right]^{-1} \mathbf{e} \left[\phi_{\hat{X}}(z) - 1\right] + 1 \tag{11}$$

The first two moments of R are:

$$\mathrm{E}[\hat{R}] = \mathbf{w} \left[\mathbf{I} - \phi_{\hat{X}}(\mathbf{A_0})\right]^{-1} \mathbf{e}\, \mathrm{E}[\hat{X}] \tag{12}$$

$$\mathrm{E}[\hat{R}^2] = \mathbf{w} \left[\mathbf{I} - \phi_{\hat{X}}(\mathbf{A_0})\right]^{-1} \mathbf{e}\, \mathrm{E}[\hat{X}^2] + 2\mathbf{w} \left[\mathbf{I} - \phi_{\hat{X}}(\mathbf{A_0})\right]^{-2} \mathbf{A}_0\, \phi'_{\hat{X}}(\mathbf{A}_0) \mathbf{e}\, \mathrm{E}[\hat{X}] \tag{13}$$

To find $\mathbf{w}$, we exploit the fact that the end of the transmission of the tagged node is a renewal time for the phase process of the tagged node, under the assumptions of the model. The one-step transition probability matrix of DMAP phase between two consecutive packet transmission ends is given by:

$$\mathbf{M} = \left[\mathbf{I} - \phi_{\hat{X}}(\mathbf{A_0})\right]^{-1} \left[\phi_{\hat{X}}(\mathbf{A}) - \phi_{\hat{X}}(\mathbf{A}_0)\right] \phi_{\hat{C}}(\mathbf{A}) \tag{14}$$

It can be verified that this is a stochastic matrix, i.e., $\mathbf{Me} = \mathbf{e}$. It is also irreducible, since $\mathbf{A}$ is. The probability distribution $\mathbf{w}$ is found as the unique solution of the linear system $\mathbf{w} = \mathbf{wM}$, that satisfies the normalization constraint $\mathbf{w}\,\mathbf{e} = 1$.

The packet inter-departure time $\hat{Y}$ is the time elapsing since the completion of transmission of a given packet until the end of transmission of the next packet. It is given by:

$$\hat{Y} = \hat{R} + \hat{C} \tag{15}$$

The corresponding GF is

$$\phi_{\hat{Y}}(z) = \phi_{\hat{R}}(z) \phi_{\hat{C}}(z) \tag{16}$$

C. PROBABILITY OF TRANSMISSION

In order to find τ, we use the renewal reward theorem. Let M be defined as the number of virtual slots between two successive transmissions of the tagged node. We express τ as 1 divided by $\mathrm{E}[M]$. It is $M = N + K$ (for the definitions of N and K see Equations (6) and (10)).

It is easy to check that N has a matrix-geometric probability distribution [39]:

$$\mathcal{P}(N = h) = \mathbf{w}\, \phi_{\hat{X}}(\mathbf{A}_0)^{h-1} \left[\mathbf{I} - \phi_{\hat{X}}(\mathbf{A}_0)\right] \mathbf{e}, \quad h \geq 1. \tag{17}$$

while K has a uniform probability distribution between 1 and W_0. The mean of M is therefore

$$\mathrm{E}[M] = \mathrm{E}[N] + \mathrm{E}[K] = \mathbf{w} \left[\mathbf{I} - \phi_{\hat{X}}(\mathbf{A}_0)\right]^{-1} \mathbf{e} + \frac{W_0 + 1}{2} \tag{18}$$

We have finally:

$$\tau = \frac{1}{\mathrm{E}[M]} = \frac{1}{\mathbf{w} \left[\mathbf{I} - \phi_{\hat{X}}(\mathbf{A}_0)\right]^{-1} \mathbf{e} + \frac{W_0+1}{2}}. \tag{19}$$

Note that $\tau_{\mathrm{sat}} = 2/(W_0 + 1)$ is the probability of transmission in a virtual slot in saturation. It can be checked that $\tau \to 0$ as $\hat{\lambda} \to 0$ (light traffic regime), while $\tau \to 2/(W_0+3)$ for $\hat{\lambda} \to \infty$ (heavy traffic regime).[2]

The transmission probability τ is found by solving a fixed point equation, since the right hand side of Equation (19) depends on q, which in turn depends on τ. Since the non-linear equation $\tau = F(\tau)$, generated by Equation (19), defines a continuous map of the interval [0, 1] onto itself, we can appeal to Brouwer's theorem to guarantee that the fixed point exists.

D. PERFORMANCE METRICS

1) PDR, CBR AND THROUGHPUT

The Packet Delivery Ratio (PDR), i.e., the probability γ of a successful reception, conditional on a transmission attempt, is

$$\gamma = (1 - \tau)^{n-1} (1 - \mathrm{PER}), \tag{20}$$

where PER is the packet error ratio, i.e., the fraction of packets that are detected with errors, given that no collision occurred. In deriving γ, we assume that collision and successful packet detection are independent events.

[2]The limiting value is slightly lower than τ_{sat} since a node is forced to wait for the new message once it completes the transmission of a previous message. This new arrival requires at least one virtual time slot.

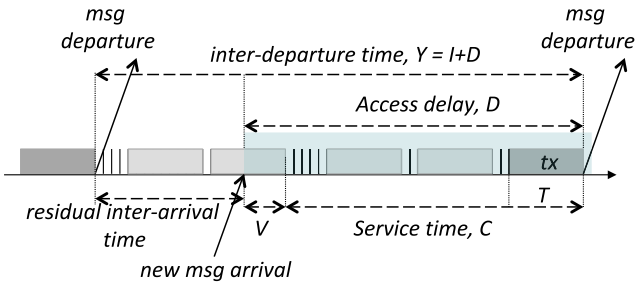

FIGURE 2. Inter-departure time and its relationship with idle time and access delay. The idle time coincides with the residual inter-arrival time.

The Channel Busy Ratio (CBR) is the average fraction of time that the channel is sensed busy by the tagged node, including time when the tagged node is transmitting. It can be expressed as:

$$\rho = \frac{b_1}{\mathrm{E}[\hat{Y}]} + \left(1 - \frac{b_1}{\mathrm{E}[\hat{Y}]}\right) \frac{\mathrm{E}[\hat{X}] - 1}{\mathrm{E}[\hat{X}]}. \tag{21}$$

We define also the normalized throughput θ, i.e., the average number of successfully delivered messages per unit time divided by the offered rate of new messages. It is

$$\theta = \frac{\gamma / \mathrm{E}[\hat{Y}]}{\hat{\lambda}}, \tag{22}$$

The throughput θ is less than 1 due to three sources of degradation: (i) message dropping upon arrival due to the node being already busy dealing with a previous message; (ii) collisions on the wireless channel; (iii) reception failure. The throughput in bit/s can be obtained by considering the average message payload L, i.e., it is $\theta_{\mathrm{bps}} = L\gamma/(\delta \mathrm{E}[\hat{Y}])$.

The coefficient of channel utilization ψ is the average fraction of channel time used successfully to deliver messages. We have

$$\psi = \frac{b_1 \gamma}{\mathrm{E}[\hat{Y}]}. \tag{23}$$

2) ACCESS DELAY

The access time $\hat{D}$ is defined as the interval between the arrival time of a message that is not dropped and the end of the transmission of that message.

Let $\hat{V}$ denote the time since message arrival until the first idle back-off slot that is counted down. After a time $\hat{V}$, the countdown of the access procedure starts (see Figure 2). The time it takes for the procedure to be completed with message transmission (including any overhead) is $\hat{C}$. Therefore, we have $\hat{D} = \hat{V} + \hat{C}$ and

$$\varphi_{\hat{D}}(z) = \phi_{\hat{C}}(z)\phi_{\hat{V}}(z). \tag{24}$$

Let us consider the virtual slot time $\hat{X}$ where an arrival occurs. The DMAP phase probability distribution at the beginning of that virtual slot time is given by $\mathbf{w}\left[\mathbf{I} - \phi_{\hat{X}}(\mathbf{A}_0)\right]^{-1}$. Given that $\hat{X} = k$, the arriving packet has to wait for h back-off slot times before seeing the end of the virtual slot time with probability

$$\mathcal{P}(\hat{V} = h | \hat{X} = k) = \mathbf{w}\left[\mathbf{I} - \phi_{\hat{X}}(\mathbf{A}_0)\right]^{-1} \mathbf{A}_0^{k-h} \mathbf{A}_1 \mathbf{A}^{h-1} \mathbf{e} \tag{25}$$

for $k \geq h$ and $h \geq 1$. This expression can be simplified by observing that $\mathbf{Ae} = \mathbf{e}$, since $\mathbf{A}$ is a stochastic matrix. Moreover, $\mathbf{A}_1\mathbf{e} = (\mathbf{A} - \mathbf{A}_0)\mathbf{e} = (\mathbf{I} - \mathbf{A}_0)\mathbf{e}$.

Removing the conditioning, we have:

$$f_{\hat{V}}(h) = \mathbf{w}\left[\mathbf{I} - \phi_{\hat{X}}(\mathbf{A}_0)\right]^{-1} \sum_{k=h}^{\infty} f_{\hat{X}}(k) \mathbf{A}_0^{k-h} (\mathbf{I} - \mathbf{A}_0)\, \mathbf{e}. \tag{26}$$

The mean value of V is

$$\mathrm{E}[\hat{V}] = \mathrm{E}[\hat{R}] - \mathbf{w}\left[\mathbf{I} - \mathbf{A}_0\right]^{-1} \mathbf{e} \tag{27}$$

Using the expressions of the mean access delay, the mean inter-departure time and the mean of $\hat{V}$, it can be verified that it is $\mathrm{E}[\hat{D}] = \mathrm{E}[\hat{Y}] - \mathbf{w}\left[\mathbf{I} - \mathbf{A}_0\right]^{-1} \mathbf{e}$. This is consistent with the fact that an inter-departure time is the sum of the residual inter-arrival time of the new message, $\mathbf{w}\left[\mathbf{I} - \mathbf{A}_0\right]^{-1} \mathbf{e}$, and of the mean access delay, $\mathrm{E}[\hat{D}]$. The illustration in Figure 2 depicts an example of inter-departure time, highlighting the relationship between the residual inter-arrival time, the residual virtual slot time $\hat{V}$, the access delay $\hat{D}$ and the inter-departure time $\hat{Y}$.

3) AGE OF INFORMATION

The AoI is the age of messages received from other nodes at the tagged node. When a message is transmitted, it has already accumulated an age corresponding to its access delay $\hat{D}$. The AoI $\hat{H}$ is akin to the excess time in a renewal process. Its CDF, given $\hat{D} = u$, is

$$\mathcal{P}(\hat{H} \leq x | \hat{D} = u) = \begin{cases} \sum_{t=0}^{x-u} \dfrac{1 - F_{\hat{Z}}(t)}{\mathrm{E}[\hat{Z}]} & x \geq u, \\ 0 & \text{otherwise}, \end{cases} \tag{28}$$

Here $\hat{Z}$ is the time between the reception of two consecutive *successful* messages from a given node. We have

$$\hat{Z} = \sum_{i=1}^{J} \hat{Y}(i) \tag{29}$$

where $\mathcal{P}(J = k) = (1 - \gamma)^{k-1}\gamma$, $k \geq 1$. The mean of $\hat{Z}$ is $\mathrm{E}[\hat{Z}] = \mathrm{E}[J]\mathrm{E}[\hat{Y}] = \mathrm{E}[\hat{Y}]/\gamma$, while the GF is given by

$$\phi_{\hat{Z}}(z) = \frac{\gamma \phi_{\hat{Y}}(z)}{1 - (1 - \gamma)\phi_{\hat{Y}}(z)}, \tag{30}$$

Noting that $\hat{D}$ is independent of $\hat{Z}$, under the assumptions of our model, and removing the conditioning in Equation (28), we get

$$F_{\hat{H}}(x) = \mathcal{P}(\hat{H} \leq x) = \sum_{u=0}^{x} f_{\hat{D}}(u) \sum_{t=0}^{x-u} \frac{1 - F_{\hat{Z}}(t)}{\mathrm{E}[\hat{Z}]}. \tag{31}$$

The GF of the PDF of $\hat{H}$ can be derived as

$$\phi_{\hat{H}}(z) = \phi_{\hat{D}}(z)\frac{1-\phi_{\hat{Z}}(z)}{(1-z)\mathrm{E}[\hat{Z}]} = \phi_{\hat{D}}(z)\frac{\gamma\left[1-\phi_{\hat{Y}}(z)\right]}{(1-z)\mathrm{E}[\hat{Y}]\left[1-(1-\gamma)\phi_{\hat{Y}}(z)\right]} \quad (32)$$

The mean AoI is calculated by deriving Equation (32) and setting $z = 1$:

$$\mathrm{E}[\hat{H}] = \mathrm{E}[\hat{D}] + \frac{\mathrm{E}[\hat{Y}^2]}{2\mathrm{E}[\hat{Y}]} - \frac{1}{2} + \mathrm{E}[\hat{Y}]\left(\frac{1}{\gamma} - 1\right). \quad (33)$$

We consider also the Peak AoI, denoted with $\hat{H}_{\mathrm{P}}$, that is the maximum age of data stored at a node, attained immediately before the reception of a successful update message. It is easy to check that $\hat{H}_{\mathrm{P}} = \hat{D} + \hat{Z}$. Therefore, we have

$$\mathrm{E}[\hat{H}_{\mathrm{P}}] = \mathrm{E}[\hat{D}] + \mathrm{E}[\hat{Z}] = \mathrm{E}[\hat{D}] + \frac{\mathrm{E}[\hat{Y}]}{\gamma}. \quad (34)$$

Comparing the Peak AoI and the expression of the mean AoI, it is apparent that

$$\mathrm{E}[\hat{H}] - \mathrm{E}[\hat{H}_{\mathrm{P}}] = \frac{\mathrm{E}[\hat{Y}^2]}{2\mathrm{E}[\hat{Y}]} - \frac{1}{2} - \mathrm{E}[\hat{Y}] = \mathrm{E}[\hat{Y}_{\mathrm{res}}] - \mathrm{E}[\hat{Y}] \quad (35)$$

where $\hat{Y}_{\mathrm{res}}$ is the residual inter-departure time. Let the Coefficient of Variation (CoV) C_Y of $\hat{Y}$ be defined as the ratio of the standard deviation of $\hat{Y}$ to the mean of $\hat{Y}$. It is well know from renewal theory (inspection paradox) that $C_Y < 1$ implies that the mean of $\hat{Y}_{\mathrm{res}}$ is less than the mean of $\hat{Y}$ ($\hat{Y}$ is said to be a smooth random variable). Conversely, for $C_Y > 1$, the mean of $\hat{Y}_{\mathrm{res}}$ is larger than the mean of $\hat{Y}$ (peaked random variable). In case of bursty message arrivals, we are in the case where $C_Y > 1$, hence the mean AoI turns out to be larger than the Peak AoI, making the name of the latter somewhat misleading. This seemingly paradoxical outcome is analogous to inspection paradox in renewal process theory. When evaluating the mean Peak AoI a large sample of $\hat{Z}$ (the time required to deliver a successful update) has the same weight as a small sample of $\hat{Z}$ in the mean. On the contrary, in the evaluation of the mean AoI, a large $\hat{Z}$ means that AoI is large for a long time, while in case of a small value of $\hat{Z}$ the small value of the AoI only weighs for a short time. In other words, the mean AoI is a time average that emphasizes the large deviations of the successful delivery time $\hat{Z}$. When the delivery process is bursty, this leads to a larger value for the mean AoI with respect to the Peak AoI. Note that, in case of geometric arrivals ($C_Y = 1$), the mean residual inter-departure time coincides with the mean inter-departure time, hence mean AoI and Peak AoI lead to the same result.

E. GENERALIZATION TO VARIABLE TRANSMISSION TIMES

In this section we outline the extension to variable transmission times. It is assumed that transmission time T has a general discrete PDF, i.e., $T = T_{\mathrm{oh}} + U$, where $U \in \{a_1, \ldots, a_\ell\}$ is the payload transmission time, ℓ being the number of different values of the payload transmission times. The indexing of the payload transmission times is defined so that $a_1 < \cdots < a_\ell$. Consistently, we also define the normalized transmission time $\hat{T} = T/\delta$, and assume that $\hat{T}$ is an integer. In the variable transmission time setting, $\hat{T} \in \{b_1, \ldots, b_\ell\}$, where $b_j = (T_{\mathrm{oh}} + a_j)/\delta$. The transmission time PDF is denoted with $f_{\hat{T}}(j) = \mathcal{P}(\hat{T} = b_j)$, while the corresponding CDF is denoted with $F_{\hat{T}}(j) = \mathcal{P}(\hat{T} \le b_j) = \sum_{i=1}^{j} f_{\hat{T}}(i)$, for $j = 1, \ldots, \ell$.

The virtual time slot duration as seen by the tagged node is still denoted with $\hat{X}$. For those virtual time slots where the tagged node does not attempt transmission, given that k nodes other than the tagged one transmit, we have

$$\hat{X} = \begin{cases} 1 & k = 0, \\ 1 + \max\{\hat{T}_1, \ldots, \hat{T}_k\} & k = 1, \ldots, n-1. \end{cases} \quad (36)$$

The probability that k nodes other than the tagged one transmit is

$$P_k = \binom{n-1}{k}\tau^k(1-\tau)^{n-1-k}, \; k = 0, 1, \ldots, n-1 \quad (37)$$

The probability that $\hat{X}$ does not exceed $1 + b_j$ is denoted with $E_j = \mathcal{P}(\hat{X} \le 1 + b_j)$, for $j = 1, \ldots, \ell$. It is derived from Equations (36) and (37) as follows:

$$\begin{aligned} E_j &= P_0 + \sum_{k=1}^{n-1} P_k \mathcal{P}(\max\{\hat{T}_1, \ldots, \hat{T}_k\} \le b_j) \\ &= (1-\tau)^{n-1} + \sum_{k=1}^{n-1}\binom{n-1}{k}\tau^k(1-\tau)^{n-1-k}F_{\hat{T}}(j)^k \\ &= (1 - \tau + \tau F_{\hat{T}}(j))^{n-1} \end{aligned}$$

Then, the probability distribution of $\hat{X}$ is given by

$$\mathcal{P}(\hat{X} = 1) = (1-\tau)^{n-1} \quad (38)$$

$$\mathcal{P}(\hat{X} = 1 + b_j) = E_j - E_{j-1}, \; j = 1, \ldots, \ell, \quad (39)$$

where we let $F_{\hat{T}}(0) = 0$, and hence $E_0 = (1-\tau)^{n-1}$, for ease of notation.

The duration $\hat{X}'$ of the virtual slot time where the tagged node attempts its transmission, given that other k nodes transmit simultaneously, is given by

$$\hat{X}' = \begin{cases} 1 + \hat{T} & k = 0, \\ 1 + \max\{\hat{T}, \hat{T}_1, \ldots, \hat{T}_k\} & k = 1, \ldots, n-1. \end{cases} \quad (40)$$

where $\hat{T}$ is the normalized transmission time of the tagged node. Following the same analysis as with $\hat{X}$, it is found for $j = 1, \ldots, \ell$:

$$\mathcal{P}(\hat{X}' = 1 + b_j) = F_{\hat{T}}(j)E_j - F_{\hat{T}}(j-1)E_{j-1}. \quad (41)$$

for $j = 1, \ldots, \ell$.

The GFs of the PDF of $\hat{X}$ is (see Equation (4))

$$\phi_{\hat{X}}(z) = qz + \sum_{j=1}^{\ell}(E_j - E_{j-1})z^{b_j+1}, \quad (42)$$

while for $\hat{X}'$ we have:

$$\phi_{\hat{X}'}(z) = \sum_{j=1}^{\ell} \left[F_{\hat{T}}(j)E_j - F_{\hat{T}}(j-1)E_{j-1}\right] z^{b_j+1}. \quad (43)$$

All expressions obtained in the fixed transmission time analysis carry over to the variable transmission time case by replacing the PDF and GF of the virtual slot time $\hat{X}$ with the generalized one in Equation (38), and the virtual slot time consisting of the fixed transmission time of the tagged node $b_1 + 1$ with $\hat{X}'$. More in depth, the definition of the service time is modified to[3] $\hat{C} = \sum_{j=1}^{K-1} \hat{X}(j) + \hat{X}'$, while nothing changes for $\hat{R}$ and $\hat{Y}$.

Performance metrics maintain their expressions, except slight modifications for the CBR and the utilization coefficient. They become respectively

$$\rho = \frac{\mathrm{E}[\hat{X}'] - 1}{\mathrm{E}[\hat{Y}]} + \left(1 - \frac{\mathrm{E}[\hat{X}'] - 1}{\mathrm{E}[\hat{Y}]}\right) \frac{\mathrm{E}[\hat{X}] - 1}{\mathrm{E}[\hat{X}]} \quad (44)$$

and

$$\psi = \mathrm{E}[\hat{T}]\gamma / \mathrm{E}[\hat{Y}]. \quad (45)$$

The expression of the PDF of AoI must be modified as well. We let $\hat{C} = \hat{W} + \hat{X}'$, where $\hat{W}$ is the countdown time. We denote the virtual slot time $\hat{X}'$, conditional on a collision, with $\hat{X}'_c$, while $\hat{X}'_s$ denotes the virtual slot time $\hat{X}'$ conditional on a successful attempt. The latter reduces to $\hat{X}'_s = 1 + \hat{T}$, while $\hat{X}'_c$ must account for the multiple transmissions leading to a collision, including the transmission of the tagged node.

The time elapsing between two successful transmissions of the tagged node is

$$\hat{Z} = \sum_{j=1}^{J-1} \left[\hat{R}(j) + \hat{W}(j) + \hat{X}'_c(j)\right] + \hat{R}(J) + \hat{W}(J) + \hat{X}'_s, \quad (46)$$

where J is a geometric random variable with PDF given by $\mathcal{P}(J = k) = (1-\gamma)^{k-1}\gamma,\ k \geq 1$.

The GF of $\hat{Z}$ is obtained as:

$$\phi_{\hat{Z}}(z) = \sum_{k=1}^{\infty} (1-\gamma)^{k-1}\gamma F_c^{k-1}(z) F_s(z) = \frac{\gamma F_s(z)}{1 - (1-\gamma)F_c(z)},$$

where

$$F_c(z) = \phi_{\hat{R}}(z) \frac{1 - [\phi_{\hat{X}}(z)]^{W_0}}{W_0\left[1 - \phi_{\hat{X}}(z)\right]} \phi_{\hat{X}'_c}(z) \quad (47)$$

$$F_s(z) = \phi_{\hat{R}}(z) \frac{1 - [\phi_{\hat{X}}(z)]^{W_0}}{W_0\left[1 - \phi_{\hat{X}}(z)\right]} \sum_{j=1}^{\ell} z^{b_j+1} f_{\hat{T}}(j). \quad (48)$$

[3]We assume that a tagged node MAC layer entity is blocked and does not accept new messages from upper layer, until the channel is first sensed idle after the end of transmission of the tagged node. If no collision occurs, this means that the MAC layer entity opens up its gate as soon as it ends its transmission. If instead there is a collision and transmissions of other colliding nodes last more than the tagged node transmission, then the tagged node gate stays closed until all concurrent transmissions die out.

There remains to give the expression of $\phi_{\hat{X}'_c}(z)$. It is

$$\phi_{\hat{X}'_c}(z) = \sum_{j=1}^{\ell} z^{b_j+1}[E_c(j) - E_c(j-1)] \quad (49)$$

with $E_c(0) = 0$ and

$$E_c(j) = F_{\hat{T}}(j) \frac{\left(1 - \tau + \tau F_{\hat{T}}(j)\right)^{n-1} - (1-\tau)^{n-1}}{1 - (1-\tau)^{n-1}} \quad (50)$$

for $j = 1, \ldots, \ell$.

Once the GF of the PDF of $\hat{Z}$ is computed, the expression of the GF of the AoI $\hat{H}$ is the same as already found for the fixed transmission time case, except that the access delay must be computed by using the generalized expression of $\phi_{\hat{X}}(z)$.

V. NUMERICAL RESULTS AND MODEL VALIDATION

We consider a two-state DMAP modeling an ON-OFF source. We characterize the node message source by means of three parameters: the mean size of a burst of messages, $\bar{b}$, the activity factor (i.e., the average fraction of time that the source is active), p_{on}, and the mean message sending time $\hat{S} = 1/\hat{\lambda}$. Then the mean duration of the ON and OFF times (i.e., time intervals when messages are generated and time intervals when the source is idle, respectively) are $\hat{T}_{\mathrm{on}} = p_{\mathrm{on}}\bar{b}\hat{S}$ and $\hat{T}_{\mathrm{off}} = (1 - p_{\mathrm{on}})\bar{b}\hat{S}$. The phase process associated with the DMAP has two states, OFF and ON. Its one-step transition probability matrix is

$$\mathbf{A} = \begin{bmatrix} 1 - 1/\hat{T}_{\mathrm{off}} & 1/\hat{T}_{\mathrm{off}} \\ 1/\hat{T}_{\mathrm{on}} & 1 - 1/\hat{T}_{\mathrm{on}} \end{bmatrix} \quad (51)$$

The matrix $\mathbf{A}_1$ is given by

$$\mathbf{A}_1 = \mathbf{D} \cdot \mathbf{A} = \begin{bmatrix} 0 & 0 \\ 0 & a_{\mathrm{on}} \end{bmatrix} \begin{bmatrix} 1 - 1/\hat{T}_{\mathrm{off}} & 1/\hat{T}_{\mathrm{off}} \\ 1/\hat{T}_{\mathrm{on}} & 1 - 1/\hat{T}_{\mathrm{on}} \end{bmatrix} \quad (52)$$

where $a_{\mathrm{on}} = 1/(p_{\mathrm{on}}\hat{S})$. The matrix $\mathbf{A}_0$ is given by $\mathbf{A}_0 = \mathbf{A} - \mathbf{A}_1$. The stationary probability vector is $\pi = [1 - p_{\mathrm{on}}, p_{\mathrm{on}}]$.

In the following, we fix $\bar{b} = 3$ and $p_{\mathrm{on}} = 1/3$, while $S = \hat{S}\,\delta$ varies in the range between 1–100 ms. The packet payload is fixed to 500 Byte. The resulting transmission time with IEEE 802.11p, including all overheads (preamble, MAC header, AIFS), assuming an air bit rate of 6 Mbit/s, is $T = 0.8\,\mathrm{ms} = 62 \cdot \delta$, where $\delta = 13\,\mu\mathrm{s}$ is the back-off slot time. It is therefore $b_1 = 62$. The packet error ratio is assumed to be PER = 0.1.

Simulations are obtained by means of a script realized in MATLAB®. The simulation model reproduces all details of the IEEE 802.11p MAC protocol, including post-back-off and immediate transmission, when a node resumes from idle state and finds an idle channel for at least an AIFS time.

Figure 3 compares the AoI metric predicted by the model with simulations. Figure 3a plots the mean AoI as a function of the message generation time S for $n = 10$ nodes. The mean AoI as a function of the number of nodes for $S = 50$ ms is shown in Figure 3b. The Peak AoI is plotted in Figure 3c as

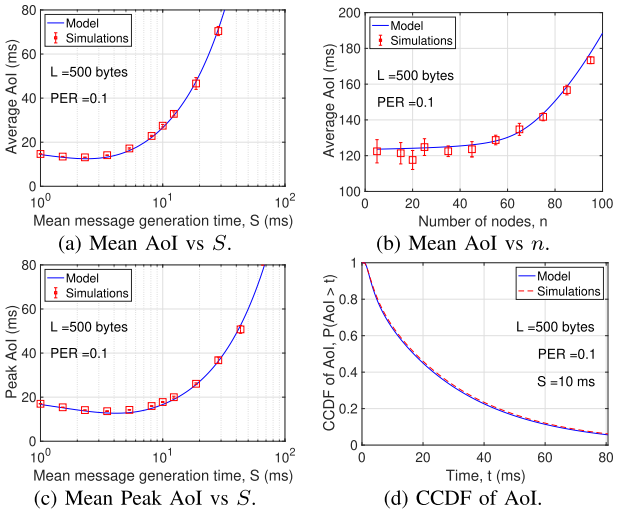

FIGURE 3. **(a) Mean AoI as a function of the message generation time. (b) mean AoI as a function of the number of nodes. (c) Mean Peak AoI as a function of the message generation time. [square markers denote simulations, with 95% confidence intervals] (d) CCDF of the AoI for message generation time $S = 10$ ms (solid blue line: model; dashed red line: simulations).**

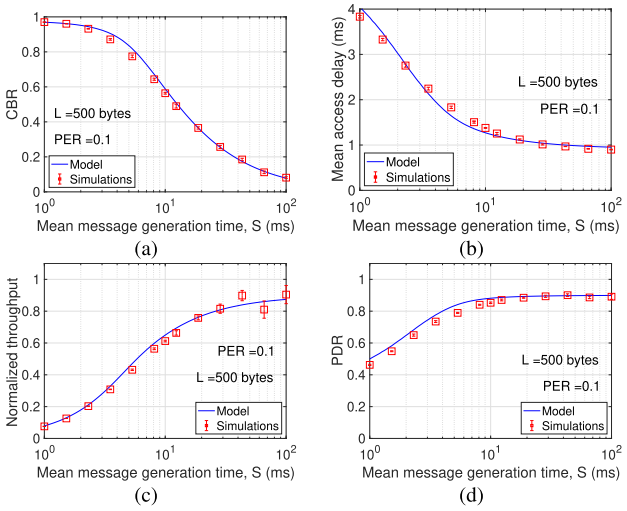

FIGURE 4. **Throughput and delay performance as a function of the mean message generation time S: (a) CBR; (b) Mean access delay; (c) Normalized throughput; (d) PDR. (square markers denote simulations with 95% confidence intervals).**

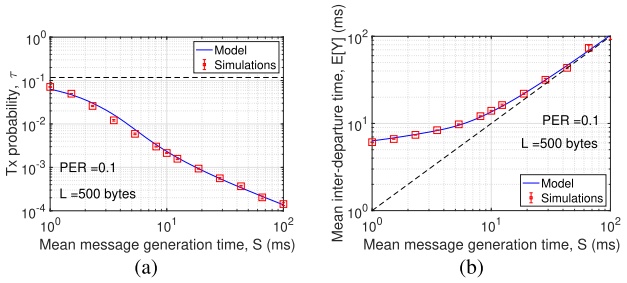

FIGURE 5. **(a) Probability of transmission τ as a function of message generation time S. (b) mean inter-departure time E[Y] as a function of message generation time S. (square markers denote simulations, with 95% confidence intervals).**

a function of S. The CCDF of the AoI for $n = 10$ nodes and $S = 10$ ms is shown in Figure 3d. In all cases, the agreement between model results and simulations is very good. As expected, the mean AoI as a function of S exhibits a minimum, i.e., there is an optimal value of the message sending rate $\lambda = 1/S$.

An interesting remark stems from the comparison of the mean AoI and the Peak AoI. It is apparent that the latter bears smaller values as the message generation time S grows. For large values of S, the dominant cause of packet loss comes from the decoding error floor (the assumed PER value), while collisions are rare. Hence, the second moment of the inter-departure time that differentiates the mean AoI and the Peak AoI has a dominant weight among all contributes. This is a consequence of the burstiness of the ON-OFF message generation process.

CBR, mean access delay, normalized throughput and PDR are plotted in Figure 4 as a function of S for $n = 10$. Qualitatively similar behavior of these metrics are obtained for other values of the parameters, e.g., number of nodes and message payload length.

Besides the high accuracy of the model, it is apparent that the system moves from a highly congested channel to a lightly loaded channel when the message generation rate $\lambda = 1/S$ decreases from 1000 msg/s down to 10 msg/s. There is a kind of phase transition phenomenon when the rate λ is varied, as evidenced by the behavior of the CBR. It can be noted also that the mean access delay is generally negligible, except when a heavy load is generated, pushing the system towards saturation.

Two important model variables are plotted in Figure 5. The transmission probability is shown in Figure 5a while the mean inter-departure time is plotted in Figure 5b. Besides the very good model accuracy, we see that τ tends to the saturation value (the level marked by the dashed horizontal line) as λ grows (to the left of the plot). Conversely, when λ gets small (to the right of the plots), the mean inter-departure time tends to coincide with $S = 1/\lambda$. This is due to the fact that packet dropping becomes negligible, so that most packets get through shortly after their arrivals.

In Figure 6 we compare the AoI of three model configurations: DMAP arrivals and fixed transmission times (left), Geometric arrivals and fixed transmission times (middle), Geometric arrivals and variables transmission times (right). Plots in top row represent the mean AoI as a function of the message generation time S. Middle row plots show the CCDF of AoI for $S = 10$ *ms*. Bottom row plots show sample paths of AoI. Plots in the first column are obtained with DMAP arrival model, while plots in the second and third columns use Geometric arrivals. The first two columns assume constant transmission times, while the rightmost column considers variable transmission times.

Geometric arrivals are a special case of DMAP, obtained by letting $\mathbf{A}_0 = [a_0]$ and $\mathbf{A}_1 = [1 - a_0]$, where $a_0 = e^{-\lambda\delta} \approx 1 - \lambda\delta$ is the probability of no arrivals in a back-off slot.

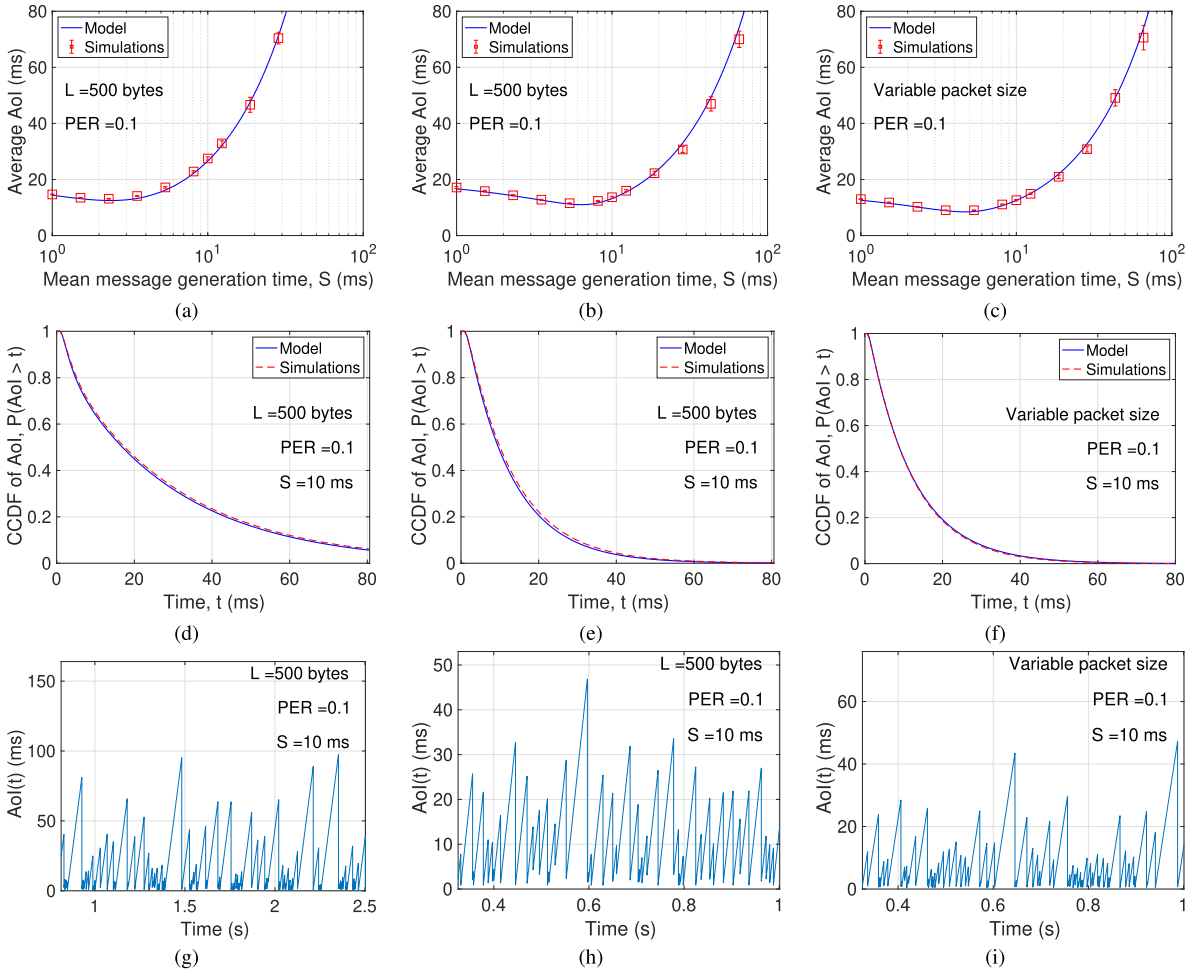

FIGURE 6. Mean AoI (top row), CCDF of AoI (middle row), and sample path of AoI for $S = 10$ ms for three model configurations: DMAP with fixed transmission times (left column), Geometric arrivals with fixed transmission times (middle column), Geometric arrivals with variable transmission times (right column). (square markers denote simulations with 95% confidence intervals).

As for variable transmission times, message lengths and relevant probabilities of occurrence are derived from the empirical model presented in [35]. Packet payload lengths are 200, 300, 330, 360, 455, 480, 600 and 800 Byte, and the corresponding probability distribution is [0.35, 0.15, 0.15, 0.15, 0.05, 0.05, 0.05, 0.05].

First, we underline once more how accurate the model turns out to be, not only for mean AoI, but also for the entire probability distribution of AoI. The behavior of the mean AoI as a function of S points out that there exists an optimal value of S, i.e., a message generation time that strikes an optimal balance between the load on the wireless channel (and hence collisions) and maintaining a sufficiently high rate of update.

The CCDFs show a relatively slow decay, so that quantiles of AoI might be quite bigger than the mean AoI. To appreciate the plots of CCDFs it is to be noted that the mean AoI in case of DMAP is 27 ms, in case of Poisson arrivals with fixed transmission times it is 13.43 ms, in case of Poisson arrivals with variable transmission times is 13.47 ms. This suggests that the mean AoI is possibly not enough when dealing with critical safety messages. AoI limit violation probabilities should be evaluated, by using the probability distribution of the AoI. It is therefore crucial to have an efficient and accurate tool to evaluate the probability distribution of the AoI, as enabled by the model defined in this work. Under this respect, it is important to underline that the numerical complexity of the evaluation of the model, including the numerical inversion of GFs, is small. It scales nicely both with n and S.

Finally, sample paths of the AoI are shown in the bottom line of plots in Figure 6. These plots point out that bursty arrivals due to ON-OFF sources generate a bursty behavior of the AoI profile, as opposed to the simple Geometric arrival process. The burstiness of the AoI is highlighted by sequences of small peaks interleaved with quite large peaks in case of DMAP arrivals.[4]

[4]Compare the y-axis scales of Figure 6g with those in Figure 6h and Figure 6i.

VI. ASYMPTOTIC ANALYSIS AND OPTIMIZATION

Building on the model, we aim at shedding light onto the optimization of AoI. To this end, we follow a three step strategy. First, we consider an asymptotic regime for $n \to \infty$, i.e., we consider large networks, and we find out the leading terms of the main model variables in that asymptotic regime. Our main purpose in this first step (Section VI-A) is to show that, at least asymptotically as n grows, the mean AoI is minimized for that arrival rate $\hat{\lambda}$ that maximizes the utilization coefficient ψ defined in Equation (23).

Second, once established the link between $\mathrm{E}[\hat{H}]$ and ψ, we find out what is the value of $\hat{\lambda}$ that maximizes ψ in the asymptotic regime in Section VI-B.

Third, leveraging on the asymptotic analysis, we provide an approximate expression of the optimized mean AoI, that turns out to be accurate for essentially any n.

The value of the presented analysis lies in the insight it provides as well as in the possibility to obtain an explicit accurate formula of the mean AoI which helps understanding the impact of key system parameters (message payload length, arrival pattern), as discussed in Section VI-C.

A. ASYMPTOTIC EXPANSION

To study the optimization of mean AoI in the asymptotic regime as $n \to \infty$, we let $\mathbf{A}_1 = \mathbf{K}_1/n$ and hence $\mathbf{A}_0 = \mathbf{A} - \mathbf{A}_1 = \mathbf{A} - \mathbf{K}_1/n$. Since it is $\hat{\lambda} = \pi\mathbf{A}_1\mathbf{e} = \pi\mathbf{K}_1\mathbf{e}/n$, the mean arrival rate per node scales inversely proportional to the number of nodes n, so that the aggregate arrival rate from all nodes is a constant. This allows us to study the asymptotic regime of large networks, maintaining the overall load on the channel at a finite, given level.

Before identifying the AoI and utilization metrics in the asymptotic regime, we need to establish a preliminary result, namely the asymptotic behavior of the mean number of virtual slot times in an idle time R (see Equation (10)). From Equation (17), we find:

$$\mathrm{E}[N] = \mathbf{w}[\mathbf{I} - \phi_{\hat{X}}(\mathbf{A}_0)]^{-1}\mathbf{e} \tag{53}$$

Let η_i, $\mathbf{u}_i$ and $\mathbf{v}_i$ denote the eigenvalues, right- and left-eigenvectors of $\mathbf{A}_0$, respectively, for $i = 1, \ldots, r$. Since $\mathbf{A}_0$ is sub-stochastic, all eigenvalues have modulus strictly less than 1. Hence it is also $|\phi_{\hat{X}}(\eta_i)| < 1$. Then, we have

$$\mathrm{E}[N] = \sum_{i=1}^{r} \frac{\mathbf{w}\,\mathbf{u}_i\,\mathbf{v}_i\,\mathbf{e}}{1 - \phi_{\hat{X}}(\eta_i)} \tag{54}$$

all terms in the summation being finite.

In the following, we assume that eigenvalues are labeled as $|\eta_1| \geq |\eta_2| \geq \cdots \geq |\eta_r|$, so that η_1 is the dominant eigenvalue. Since $\mathbf{A}$ is the one-step transition probability matrix of an irreducible finite Markov chain, the eigenvalues of $\mathbf{A}$ have modulus less or equal to 1 and only a single eigenvalue equals 1 (this is the dominant eigenvalue, if we restrict our attention to aperiodic Markov chains). The right and left eigenvectors of $\mathbf{A}$ corresponding to the eigenvalue 1 are $\mathbf{e}$ and π respectively. As n grows, $\mathbf{A}_0 = \mathbf{A} - \mathbf{K}_1/n$ tends to $\mathbf{A}$, hence the dominant eigenvalue of $\mathbf{A}_0$, namely η_1, tends to the dominant eigenvalue of $\mathbf{A}$, that is to say 1. Consistently, the left and right eigenvectors of $\mathbf{A}_0$ associated with η_1, namely $\mathbf{v}_1$ and $\mathbf{u}_1$, tend to π and $\mathbf{e}$ respectively. In the following we derive the asymptotic expansion to the first order of these quantities, as $n \to \infty$.

We characterize the leading term of the asymptotic expansion of $\eta_1, \mathbf{u}_1$ and $\mathbf{v}_1$, by equating the constant terms and terms inversely proportional to n in the identities $\mathbf{A}_0\mathbf{u}_1 = \eta_1\mathbf{u}_1$ and $\mathbf{v_1}\mathbf{A}_0 = \eta_1\mathbf{v}_1$. Considering the former identity, we have

$$\left(\mathbf{A} - \frac{\mathbf{K}_1}{n}\right)\left(\mathbf{e} - \frac{\delta\mathbf{u}_1}{n}\right) = \left(1 - \frac{\hat{\kappa}}{n}\right)\left(\mathbf{e} - \frac{\delta\mathbf{u}_1}{n}\right). \tag{55}$$

Since $\mathbf{A}\mathbf{e} = \mathbf{e}$ ($\mathbf{A}$ is stochastic), equating the terms inversely proportional to n, we get

$$\mathbf{A}\,\delta\mathbf{u}_1 + \mathbf{K}_1\mathbf{e} = \hat{\kappa}\mathbf{e} + \delta\mathbf{u}_1. \tag{56}$$

from which it can be found that

$$\delta\mathbf{u}_1 = (\mathbf{I} - \mathbf{A} + \mathbf{e}\pi)^{-1}\mathbf{K}_1\mathbf{e}. \tag{57}$$

Analogously, we have

$$\delta\mathbf{v}_1 = \pi\mathbf{K}_1(\mathbf{I} - \mathbf{A} + \mathbf{e}\pi)^{-1}. \tag{58}$$

Pre-multiplying Equation (56) by π, it is easily found that $\hat{\kappa} = \pi\mathbf{K}_1\mathbf{e}$. Note that $\hat{\lambda} = \pi\mathbf{A}_1\mathbf{e} = \pi\mathbf{K}_1\mathbf{e}/n = \hat{\kappa}/n$. It is seen that the coefficient $\hat{\kappa}$ is tied to the mean arrival rate asymptotic expansion. More in depth, $\hat{\kappa} = n\hat{\lambda}$ is the aggregate (normalized) arrival rate of messages to all nodes.

Summing up, the asymptotic expansions of the dominant eigenvalue of $\mathbf{A}_0$ and its eigenvectors as $n \to \infty$ is given as follows:

$$\eta_1 \sim 1 - \frac{\hat{\kappa}}{n} \tag{59}$$

$$\mathbf{u}_1 \sim \mathbf{e} - \frac{1}{n}(\mathbf{I} - \mathbf{A} + \mathbf{e}\pi)^{-1}\mathbf{K}_1\mathbf{e} \tag{60}$$

$$\mathbf{v}_1 \sim \pi - \frac{1}{n}\pi\mathbf{K}_1(\mathbf{I} - \mathbf{A} + \mathbf{e}\pi)^{-1} \tag{61}$$

As $n \to \infty$, all summands in Equation (54) remain bounded, except the term corresponding to $i = 1$. In that special case we have $\lim_{n\to\infty} \phi_{\hat{X}}(\eta_1) = \phi_{\hat{X}}(1) = 1$, while for all $i \neq 1$ we have $\lim_{n\to\infty} \phi_{\hat{X}}(\eta_1) \neq 1$ (it is actually $\lim_{n\to\infty} |\phi_{\hat{X}}(\eta_1)| < 1$), since η_i, $i = 2, \ldots, n$, converge to eigenvalues of $\mathbf{A}$ different from 1.

As a result, in the limiting regime, the sum in Equation (54) is dominated by the term with $i = 1$, and we can use the asymptotic expansions of η_1, $\mathbf{u}_1$ and $\mathbf{v}_1$. We have

$$\mathrm{E}[N] \sim \frac{\mathbf{w}\mathbf{u_1}\,\mathbf{v_1}\mathbf{e}}{1 - \phi_{\hat{X}}(\eta_1)} = \frac{\left(\mathbf{we} - \frac{\mathbf{w}\delta\mathbf{u}_1}{n}\right)\left(\pi\mathbf{e} - \frac{\delta\mathbf{v}_1\mathbf{e}}{n}\right)}{1 - \phi_{\hat{X}}\left(1 - \frac{\hat{\kappa}}{n}\right)}. \tag{62}$$

It is $\mathbf{we} = \pi\mathbf{e} = 1$. Moreover, expanding $\phi_{\hat{X}}(\cdot)$ in series with starting point 1, we have

$$\phi_{\hat{X}}\left(1 - \frac{\hat{\kappa}}{n}\right) \sim \phi_{\hat{X}}(1) - \phi'_{\hat{X}}(1)\frac{\hat{\kappa}}{n} = 1 - \mathrm{E}[\hat{X}]\frac{\hat{\kappa}}{n}. \tag{63}$$

Substituting into Equation (62), we get

$$\begin{aligned}\mathrm{E}[N] &\sim \frac{n}{\hat{\kappa}\,\mathrm{E}[\hat{X}]}\left(1-\frac{\mathbf{w}\delta\mathbf{u}_1+\delta\mathbf{v}_1\mathbf{e}}{n}\right)\\ &\sim \frac{n}{\hat{\kappa}\,\mathrm{E}[\hat{X}]}+\text{constant}\end{aligned} \tag{64}$$

Since $\lim_{n\to\infty}\mathbf{w}=\pi$, it is $\mathbf{w}\delta\mathbf{u}_1\to\hat{\kappa}$. It is also easy to check that $\delta\mathbf{v}_1\mathbf{e}=\hat{\kappa}$. Then, the constant appearing in Equation (64) equals $-2/\mathrm{E}[\hat{X}]$.

Looking at the expressions of the first two moments of R, it is easy to recognize that we have

$$\mathrm{E}[\hat{R}]\sim\mathrm{E}[\hat{X}]\cdot\frac{n}{\hat{\kappa}\,\mathrm{E}[\hat{X}]}=\frac{n}{\hat{\kappa}},$$

$$\mathrm{E}[\hat{R}^2]\sim\mathrm{E}[\hat{X}^2]\frac{n}{\hat{\kappa}\,\mathrm{E}[\hat{X}]}+2\left(\mathrm{E}[\hat{X}]\right)^2\frac{n^2}{\hat{\kappa}^2\left(\mathrm{E}[\hat{X}]\right)^2}\sim\frac{2\,n^2}{\hat{\kappa}^2}.$$

The transmission probability τ can be expanded in the asymptotic regime as well. We have

$$\tau=\frac{1}{\mathrm{E}[N]+\frac{W_0+1}{2}}\sim\frac{1}{\frac{n}{\hat{\kappa}\mathrm{E}[\hat{X}]}+\frac{W_0+1}{2}}\sim\frac{\hat{\kappa}\mathrm{E}[\hat{X}]}{n}. \tag{65}$$

The probability of successful message delivery becomes

$$\gamma\sim\left(1-\frac{\hat{\kappa}\mathrm{E}[\hat{X}]}{n}\right)^{n-1}(1-\mathrm{PER})\sim e^{-\hat{\kappa}\mathrm{E}[\hat{X}]}(1-\mathrm{PER}). \tag{66}$$

Since $\hat{X}$, $\hat{C}$ and $\hat{D}$ have finite support, in the limit as n grows, we have

$$\mathrm{E}[\hat{Y}]=\mathrm{E}[\hat{R}]+\mathrm{E}[\hat{C}]\sim\frac{n}{\hat{\kappa}},$$

$$\mathrm{E}[\hat{Y}^2]=\mathrm{E}[\hat{R}^2]+2\mathrm{E}[\hat{R}]\mathrm{E}[\hat{C}]+\mathrm{E}[\hat{C}^2]\sim\frac{2\,n^2}{\hat{\kappa}^2},$$

and, using the asymptotic expansion of the first two moments of $\hat{Y}$, we get

$$\mathrm{E}[\hat{H}]\sim\frac{2\,n^2/\hat{\kappa}^2}{2\,n/\hat{\kappa}}+\frac{n}{\hat{\kappa}}\left(\frac{1}{\gamma}-1\right)=\frac{n}{\hat{\kappa}\gamma}\sim\frac{\mathrm{E}[\hat{Y}]}{\gamma} \tag{67}$$

From the right-most hand side, it is seen that the mean AoI is asymptotically inversely proportional to the utilization coefficient $\psi=\mathrm{E}[\hat{T}]\gamma/\mathrm{E}[\hat{Y}]$. This proves that the mean AoI is minimized for the same value of $\hat{\lambda}$ that maximizes the utilization coefficient ψ. In other words, in the asymptotic regime as $n\to\infty$, the mean AoI is dominated by a term that is inversely proportional to the utilization coefficient. We will see that the correspondence of the location of the maximum of ψ and the minimum of $\mathrm{E}[\hat{H}]$ holds more generally, for virtually any n.

This correspondence can be checked by comparing Figure 7 with Figure 3a. In Figure 7 ψ is plotted against S for $n=10$ nodes. It peaks at a value of S that strikes an optimal balance between excessive load of the channel (hence too many collisions) and too light load of the channel, whence most of channel time goes idle.

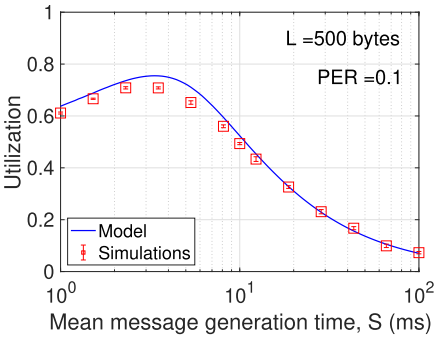

FIGURE 7. Utilization coefficient ψ as a function of the message generation time for $n=10$ nodes. (square markers denote simulations with 95% confidence intervals).

A similar connection between the extremal points of the utilization coefficient of the communication channel and the mean AoI has been observed for ALOHA-type multiple access in [40].

B. MAXIMIZATION OF THE UTILIZATION IN THE ASYMPTOTIC REGIME

To gain further insight, let us restrict to the case that the transmission time (including any overhead) is a constant $T=b_1\delta$. We also use non-normalized times in this section and in the next one, which makes results more intuitively readable.

We have $\mathrm{E}[X]=\delta+(1-q)T$ and $\mathrm{E}[X']=\delta+T$. The mean inter-departure time is the sum of the expected idle time R, the mean countdown time ($(W_0-1)/2$ times the mean virtual slot time) and a final virtual slot time where the tagged station transmits. Therefore

$$\begin{aligned}\mathrm{E}[Y]&=\mathrm{E}[R]+\frac{W_0-1}{2}\mathrm{E}[X]+\delta+T\\ &=\mathbf{w}\left[\mathbf{I}-\phi_{\hat{X}}(\mathbf{A}_0)\right]^{-1}\mathbf{e}\,\mathrm{E}[X]+\frac{W_0+1}{2}\mathrm{E}[X]+qT\\ &=\frac{\mathrm{E}[X]}{\tau}+(1-\tau)^{n-1}T=\frac{\delta+T-(1-\tau)^nT}{\tau}.\end{aligned}$$

The utilization coefficient of the wireless channel can be rewritten as

$$\begin{aligned}\psi&=\frac{T\gamma}{\mathrm{E}[Y]}=\tau\,\frac{T(1-\tau)^{n-1}(1-\mathrm{PER})}{\delta+T-(1-\tau)^nT}\\ &=\frac{\tau(1-\tau)^{n-1}}{\beta+1-(1-\tau)^n}(1-\mathrm{PER})\end{aligned} \tag{68}$$

where $\beta=\delta/T$. This expression is maximized for $\tau=\tau^*$ equal to the unique solution in (0, 1) of the equation:

$$(\beta+1)(1-n\tau)=(1-\tau)^n. \tag{69}$$

We have seen in Equation (65) that $\tau\sim\kappa\mathrm{E}[X]/n=\alpha/n$, where α is a non-dimensional constant. Substituting $\tau=\alpha/n$ into Equation (69) and letting $n\to\infty$, we have $\tau^*\sim\alpha^*/n$, where α^* is the unique solution of the equation

$$(\beta+1)(1-\alpha)=e^{-\alpha} \tag{70}$$

for $\alpha \in (0,1)$. Re-arranging terms in (70), we establish the following identity, which we will use later:

$$\alpha^*(1+\beta) = \beta + 1 - e^{-\alpha^*}. \tag{71}$$

By letting $\tau = \alpha/n$ into Equation (68), the overall channel utilization coefficient $\Psi = n\psi$ takes the following simple asymptotic expression

$$\Psi_\infty = \lim_{n\to\infty} n\psi = \frac{\alpha e^{-\alpha}}{\beta + 1 - e^{-\alpha}}(1 - \text{PER}). \tag{72}$$

This is maximized for $\alpha = \alpha^*$. From the result shown in Section VI-A, we know that $\alpha = \alpha^*$, i.e., $\tau = \tau^* = \alpha^*/n$, also minimizes asymptotically the mean AoI.

The optimal message generation rate λ^* must correspond to the optimal value of the transmission probability τ^*. In fact, it is possible to make a connection between the leading term of the asymptotic expansion of $\tau^* = \alpha^*/n$ and $\lambda = \kappa/n$, as follows:

$$\frac{\alpha^*}{n} \sim \frac{1}{\frac{W_0+1}{2} + \frac{1}{\kappa \mathrm{E}[X]/n}} \sim \frac{\kappa \mathrm{E}[X]}{n}. \tag{73}$$

Note that, in the asymptotic regime $q = (1-\alpha^*/n)^{n-1} \sim e^{-\alpha^*}$. Then, using the result in (71), we get

$$\begin{aligned}\mathrm{E}[X] &= \delta + T - qT \sim T(\beta + 1 - e^{-\alpha^*}) \\ &= T(\beta+1)\alpha^* = (\delta+T)\alpha^*.\end{aligned} \tag{74}$$

Equating the leading terms on both sides of (73) and using (74), we get

$$\frac{\alpha^*}{n} \sim \frac{\kappa \mathrm{E}[X]}{n} = \frac{\kappa(\delta+T)\alpha^*}{n}. \tag{75}$$

Hence, it must be $\kappa = 1/(\delta+T)$. Therefore, we find that the asymptotically optimal message sending rate, i.e., the one that maximizes the coefficient of utilization is:

$$\lambda^* = \frac{\kappa}{n} = \frac{1}{(\delta+T)n}. \tag{76}$$

The optimal value of the average message generation time interval is therefore equal to n times the packet transmission time. This is a simple and insightful result.

C. EXPLICIT FORMULA OF THE MEAN AoI

The mean AoI consists of the sum of three terms: the mean access delay $\mathrm{E}[D]$, the (asymptotically) dominating term that is inversely proportional to the utilization factor, $\mathrm{E}[Y]/\gamma$, and the remaining term, which is a result of the variation of the inter-departure time, $\frac{\mathrm{E}[Y^2]}{2\mathrm{E}[Y]} - \mathrm{E}[Y] - \frac{\delta}{2}$.

In the following, we find an expression for the minimum attainable value of the mean AoI, denoted with $\bar{H}^*$. According to the decomposition introduced above, we write $\bar{H}^* = \bar{D}^* + \bar{H}^*_{\text{dom}} + \bar{H}^*_{\text{var}}$. We have learned that the minimum is attained for $1/\lambda \sim n(\delta+T)$. We exploit the asymptotic results for large n, to derive approximations of the component terms of the mean AoI for the optimal value of λ.

The mean access delay is approximated with the mean service time $\mathrm{E}[C] = \frac{W_0+1}{2}\mathrm{E}[X] + qT$, whose expression is in turn obtained by approximating the probability $q = (1-\tau)^{n-1} \sim (1-\alpha^*/n)^{n-1} \approx e^{-\alpha^*}$. Then, it is $\mathrm{E}[X] \sim \delta + (1-e^{-\alpha^*})T$, and we have

$$\begin{aligned}\bar{D}^* &= e^{-\alpha^*}T + \frac{W_0+1}{2}\left[\delta + (1-e^{-\alpha^*})T\right] \\ &= \left(1 - \alpha^* + \frac{W_0+1}{2}\alpha^*\right)(\delta+T)\end{aligned} \tag{77}$$

As for the dominating term $\bar{H}^*_{\text{dom}} = \mathrm{E}[\hat{Y}]/\gamma$, we exploit the asymptotic result $\mathrm{E}[Y] \sim \mathrm{E}[R] \sim n/\kappa$. The minimum of the mean AoI is attained with $\kappa = \kappa^* = 1/(\delta+T)$. Since it is $\gamma = q(1-\text{PER}) \sim e^{-\alpha^*}(1-\text{PER})$, we have $\bar{H}^*_{\text{dom}} = \frac{n(\delta+T)}{e^{-\alpha^*}(1-\text{PER})}$.

A refined approximation can be obtained starting from the expression of the transmission probability τ and substituting the asymptotic expansions of $\tau = \alpha/n$ and $\lambda = \kappa/n$. We get

$$\frac{\alpha}{n} = \frac{1}{\frac{W_0+1}{2} + \frac{1}{\kappa \mathrm{E}[X]/n}} \tag{78}$$

Getting κ, we find

$$\kappa = \frac{\alpha/\mathrm{E}[X]}{1 - \frac{\alpha(W_0+1)}{2\,n}} \tag{79}$$

Under the optimal choice of α, we have $(\beta+1)(1-\alpha^*) = e^{-\alpha^*}$. Hence, $\mathrm{E}[X] = \delta + T - qT \sim \delta + T - e^{\alpha^*}T = \alpha^*(\delta+T)$. Substituting into Equation (79) we have

$$\kappa^* = \frac{1}{(\delta+T)\left(1 - \frac{\alpha^*(W_0+1)}{2\,n}\right)} \tag{80}$$

Finally, using Equation (66), we find

$$\bar{H}^*_{\text{dom}} = \frac{n}{\kappa^*\gamma} \sim \frac{\left(n - \alpha^*\frac{W_0+1}{2}\right)(\delta+T)}{e^{-\alpha^*}(1-\text{PER})}. \tag{81}$$

The third component of the optimal AoI is found by noting that, at least asymptotically for large n and hence small $\lambda \sim \kappa/n$, we have $Y \sim R \sim I$, where I is the residual inter-arrival time, starting from the end of a transmission. The probability that an arrival occurs after h back-off slot times is $f_I(h) = \mathcal{P}(I = h\delta) = \mathbf{w}\mathbf{A}_0^{h-1}\mathbf{A}_1\mathbf{e}$, $h \geq 1$. Then it is routine (yet long) calculation to derive that

$$\begin{aligned}\mathrm{E}[I] &= \delta\left[\mathbf{w}(\mathbf{I}-\mathbf{A}_0)^{-1}\mathbf{e}\right], \\ \mathrm{E}[I^2] &= \delta^2\left[2\mathbf{w}(\mathbf{I}-\mathbf{A}_0)^{-2}\mathbf{e} + \mathbf{w}(\mathbf{I}-\mathbf{A}_0)^{-1}\mathbf{e}\right].\end{aligned}$$

Putting all pieces together, we have the following expression for the third component of the optimal mean AoI:

$$\begin{aligned}\bar{H}^*_{\text{var}} &= \frac{\mathrm{E}[I^2]}{2\mathrm{E}[I]} - \mathrm{E}[I] - \frac{\delta}{2} \\ &= \delta\left[\frac{\mathbf{w}(\mathbf{I}-\mathbf{A}_0)^{-2}\mathbf{e}}{\mathbf{w}(\mathbf{I}-\mathbf{A}_0)^{-1}\mathbf{e}} - \mathbf{w}(\mathbf{I}-\mathbf{A}_0)^{-1}\mathbf{e}\right].\end{aligned} \tag{82}$$

There remains to find an expression for $\mathbf{w}$. The phase of the DMAP at the end of the transmission can be approximated with the phase upon an arrival, since the transmission

ends $\approx C$ time after the arrival and $C \ll I$ with high probability. Then, the following approximation can be used:

$$\mathbf{w} \approx \pi(\mathbf{I} - \mathbf{A}_0)^{-1}\mathbf{A}_1, \tag{83}$$

where π is the steady-state probability distribution of the DMAP phase. Summing up, we have

$$\bar{H}^* = \bar{D}^* + \bar{H}^*_{\text{dom}} + \bar{H}^*_{\text{var}}, \tag{84}$$

where the expressions of the three terms are given in Equations (77)and (81) to (83).

In the special case of a Geometric arrival process, it is $\mathbf{A}_0 = [a_0]$ and $\mathbf{A}_1 = [1 - a_0]$, where $a_0 = e^{-\lambda\delta} \approx 1 - \lambda\delta$. It is easy to check that the term $\bar{H}^*_{\text{var}}$ cancels out. Then, we have

$$\begin{aligned}\bar{H}^* &= \bar{D}^* + \frac{\left(n - \alpha^* \frac{W_0+1}{2}\right)(\delta + T)}{e^{-\alpha^*}(1 - \text{PER})} \\ &\approx \frac{nT}{(1 - \alpha^*)(1 - \text{PER}),}\end{aligned} \tag{85}$$

where the last approximation is justified by the fact that both the mean access delay and the offset correction $-\alpha^* \frac{W_0+1}{2}$ have a small impact on the numerical result.

The explicit expression of the optimal mean AoI is readily evaluated, given the basic parameters of the system. It provides a lower bound of the attainable AoI performance, which is actually achieved by setting the mean message generation time to $n(\delta + T)$. It also shows that the optimal mean AoI grows proportionally to the number of nodes and proportionally to the transmission time of messages.

For a numerical example, we consider a DMAP process defined by a two-state Markov chain, OFF and ON state. The mean time in ON state is 50 ms, the mean fraction of time the message source is in ON state is $p_{\text{on}} = 1/3$. It is therefore

$$\mathbf{A} = \begin{bmatrix} 0.99987 & 0.00013 \\ 0.00026 & 0.99974 \end{bmatrix} \tag{86}$$

Arrivals occur with probability $\hat{\lambda}/p_{\text{on}} = 3\hat{\lambda}$ while in ON state, with probability 0 in OFF state. Hence

$$\mathbf{A}_1 = \begin{bmatrix} 0 & 0 \\ 0 & 3\hat{\lambda} \end{bmatrix} \tag{87}$$

and $\mathbf{A}_0 = \mathbf{A} - \mathbf{A}_1$.

Transmission times are constant, equal to $T = 0.8$ ms. The normalized transmission time is $b_1 = T/\delta = 62$.

We compare the approximation derived in this section for the optimal mean AoI (curves labeled with "appx" in the plots) with three other methods to evaluate the optimal mean AoI:

- exhaustive search of the minimum of the mean AoI as obtained from the evaluation of the exact model in Section IV, i.e., not approximated with the asymptotic expansion (curves labeled with "opt" in the plots).
- evaluation of the model in Section IV for $\lambda = \frac{1}{n(\delta+T)} = \frac{1}{63\,\delta\,n}$, the supposedly optimal value of the message generation rate (curves labeled with "asy" in the plots).

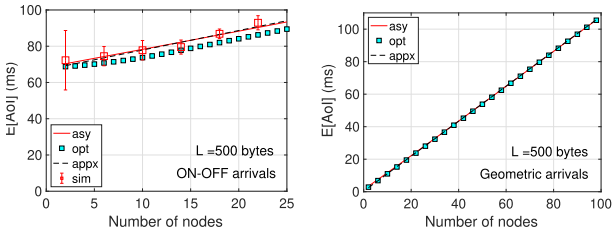

(a) DMAP arrivals (b) Geometric arrivals.

FIGURE 8. (a) optimal mean AoI as a function of the number of nodes *n* in case of ON-OFF DMAP arrivals. (b) optimal mean AoI as a function of the number of nodes *n* in case of Geometric arrivals. (red square markers in Figure 8a denote simulations with 95% confidence intervals).

- Simulations obtained by the same simulation code used in Section V.

Figure 8a shows the optimal mean AoI computed with the three approaches described above in case of DMAP arrivals and fixed transmission time. The square markers correspond to the exact optimal values, found by numerical search on the curve of $\text{E}[H]$ as a function of λ for each value of the number of nodes n. The solid line represents the value of $\text{E}[H]$ obtained from the analytical model for $\lambda = \lambda^* = 1/[n(\delta + T)]$. The dashed line shows the approximation in Equation (84). Finally, simulations are shown by means of square markers with 95%-level confidence intervals.

The good match between exact optimal values and approximations obtained from the asymptotic theory is apparent. Except of a marginal offset, it turns out that the approximation is almost exact for all considered values of n, not just asymptotically for large n.

Figure 8b compares the three analytical methods to evaluate the optimal mean AoI in case of Geometric arrivals. In this case it appears that there is an excellent match among all three methods. In other words, the simple approximation devised in Equation (85) provides an excellent prediction of the exact value computed according to the model. Moreover, it can be noted that optimal values of the mean AoI achieved under Geometric arrivals are substantially smaller than in case of DMAP. This is expected, given that ON-OFF DMAP generates message in a bursty way, thus affecting adversely timely delivery of message.

VII. CONCLUSION

Bursty traffic is a typical feature of CPS, where the generation of updates is coupled with the variability of a communicated parameter. For example, in V2X communications, mobility of a node triggers update messages with a current position of a vehicle. In this work we presented a new analytical model of a one-hop broadcast update message exchange in a CSMA network with bursty message arrivals. The model allows for the evaluation of moments and probability distributions of several metrics, including AoI. The model also lends itself to an insightful asymptotic analysis as the number of nodes grows. The asymptotic analysis suggests the optimal message update rate to minimize the mean AoI, which is shown to

coincide with the optimum of the wireless channel utilization. The simple approximation provided by the asymptotic analysis for large number of nodes is quite close to the exact optimal rate also for relatively small values of the number of nodes.

Further developments of the model can be in the direction of heterogeneous case, where nodes use different message generation rates. For this generalization we need to modify the probabilities of a specific node to transmit in a virtual time slot. These can be found by solving a system of non-linear equations with an appeal to Brouwer's theorem which guarantees an existence of the fixed point.

APPENDIX

The expression in Equation (11) is hereby derived.

Let t_0 denote the start time of the interval $\hat{R}$. Let also $\mathbf{w}$ denote an r-dimensional row vector whose i-th entry is $w_i = \mathcal{P}(J(t_0) = i)$, $i = 1, \ldots, r$, i.e., $\mathbf{w}$ is the probability distribution of DMAP phase $J(t)$ sampled at the end of packet transmission times of the tagged node.

We have for the GF of $\hat{R}$:

$$\phi_{\hat{R}}(z) = \mathrm{E}[z^{\hat{R}}] = \sum_{i=1}^{r}\sum_{j=1}^{r}\sum_{k=1}^{\infty} w_i P_{ij}(k) z^k \tag{88}$$

where

$$P_{ij}(k) = \mathcal{P}(\hat{R} = k, J(t_0 + \hat{R}) = j | J(t_0) = i) \tag{89}$$

Let $\mathbf{P}$ denote the $r \times r$ matrix whose entry (i, j) is $P_{ij}(k)$.

Conditional on $N = h$ and on $\hat{X}(j) = x_j$, $j = 1, \ldots, h$, it is $\hat{R} = k = x_1 + \ldots, x_h$. The conditioning event $N = h$ means that there is no arrival in the first $h - 1$ virtual slots, then there is at least one arrival in the h-th slot time. Under these conditioning events, it can be verified that

$$\mathbf{P} = (\mathbf{A}_0)^{x_1 + \cdots + x_{h-1}} [\mathbf{A}^{x_h} - \mathbf{A}_0^{x_h}] \tag{90}$$

Substituting into Equation (88), we have

$$\begin{aligned}
\phi_{\hat{R}}(z) &= \sum_{h=1}^{\infty}\sum_{x_1=0}^{\infty}\cdots\sum_{x_h=0}^{\infty} \mathbf{wPe}\, z^{x_1} f_{\hat{X}}(x_1)\cdots z^{x_h} f_{\hat{X}}(x_h) \\
&= \sum_{h=1}^{\infty} \mathbf{w}\,[\phi_{\hat{X}}(\mathbf{A}_0 z)]^{h-1}\left[\phi_{\hat{X}}(\mathbf{A}z) - \phi_{\hat{X}}(\mathbf{A}_0 z)\right]\mathbf{e} \\
&= \mathbf{w}\left[\mathbf{I} - \phi_{\hat{X}}(\mathbf{A}_0 z)\right]^{-1}\left[\phi_{\hat{X}}(\mathbf{A}z) - \phi_{\hat{X}}(\mathbf{A}_0 z)\right]\mathbf{e} \\
&= \mathbf{w}\left[\mathbf{I} - \phi_{\hat{X}}(\mathbf{A}_0 z)\right]^{-1}\mathbf{e}\,[\phi_{\hat{X}}(z) - 1] + 1
\end{aligned} \tag{91}$$

where

$$\phi_{\hat{X}}(\mathbf{A}_0 z) = q\mathbf{A}_0\, z + (1 - q)\mathbf{A}_0^{b_1+1}\, z^{b_1+1} \tag{92}$$

Since $\mathbf{A}_0$ is a sub-stochastic matrix, the eigenvalues of $\phi_{\hat{X}}(\mathbf{A_0}z)$ are strictly less than 1 for $|z| \leq 1$. Hence, the inverse matrix appearing in Equation (91) exists.

REFERENCES

[1] A. Correa, R. Alms, J. Gozalvez, M. Sepulcre, M. Rondinone, R. Blokpoel, L. Lücken, and G. Thandavarayan, "Infrastructure support for cooperative maneuvers in connected and automated driving," in *Proc. IEEE Intell. Vehicles Symp. (IV)*, Jun. 2019, pp. 20–25.

[2] W. Chen, J. Liu, H. Guo, and N. Kato, "Toward robust and intelligent drone swarm: Challenges and future directions," *IEEE Netw.*, vol. 34, no. 4, pp. 278–283, Jul. 2020.

[3] M. Wollschlaeger, T. Sauter, and J. Jasperneite, "The future of industrial communication: Automation networks in the era of the Internet of Things and industry 4.0," *IEEE Ind. Electron. Mag.*, vol. 11, no. 1, pp. 17–27, Mar. 2017.

[4] N. Lyamin, A. Vinel, M. Jonsson, and B. Bellalta, "Cooperative awareness in VANETs: On ETSI EN 302 637-2 performance," *IEEE Trans. Veh. Technol.*, vol. 67, no. 1, pp. 17–28, Jan. 2018.

[5] J. B. Kenney, "Dedicated short-range communications (DSRC) standards in the United States," *Proc. IEEE*, vol. 99, no. 7, pp. 1162–1182, Dec. 2011.

[6] W. Anwar, N. Franchi, and G. Fettweis, "Physical layer evaluation of V2X communications technologies: 5G NR-V2X, LTE-V2X, IEEE 802.11bd, and IEEE 802.11p," in *Proc. IEEE 90th Veh. Technol. Conf. (VTC-Fall)*, Sep. 2019, pp. 1–7.

[7] R. D. Yates, Y. Sun, D. R. Brown, S. K. Kaul, E. Modiano, and S. Ulukus, "Age of information: An introduction and survey," *IEEE J. Sel. Areas Commun.*, vol. 39, no. 5, pp. 1183–1210, May 2021.

[8] T. Linget, "White paper: C-V2X use cases volume II: Examples and service level requirements, version 1.0," 5GAA Automot. Assoc., Munich, Germany, White Paper, Oct. 2020. [Online]. Available: https://5gaa.org/wp-content/uploads/2020/10/5GAA_White-Paper_C-V2X-Use-Cases-Volume-II.pdf

[9] I. Turcanu and C. Sommer, "Poster: Potentials of mixing TSN wired networks and best-effort wireless networks for V2X," in *Proc. IEEE Veh. Netw. Conf. (VNC)*, Nov. 2021, pp. 135–136.

[10] A. Ghosal and M. Conti, "Security issues and challenges in V2X: A survey," *Comput. Netw.*, vol. 169, Mar. 2020, Art. no. 107093.

[11] S. Kaul, R. Yates, and M. Gruteser, "Real-time status: How often should one update?" in *Proc. IEEE INFOCOM*, Mar. 2012, pp. 2731–2735.

[12] Y. Inoue, H. Masuyama, T. Takine, and T. Tanaka, "A general formula for the stationary distribution of the age of information and its application to single-server queues," *IEEE Trans. Inf. Theory*, vol. 65, no. 12, pp. 8305–8324, Dec. 2019.

[13] A. M. Bedewy, Y. Sun, and N. B. Shroff, "The age of information in multihop networks," *IEEE/ACM Trans. Netw.*, vol. 27, no. 3, pp. 1248–1257, Jun. 2019.

[14] I. Kadota, A. Sinha, and E. Modiano, "Scheduling algorithms for optimizing age of information in wireless networks with throughput constraints," *IEEE/ACM Trans. Netw.*, vol. 27, no. 4, pp. 1359–1372, Aug. 2019.

[15] I. Kadota and E. Modiano, "Minimizing the age of information in wireless networks with stochastic arrivals," *IEEE Trans. Mobile Comput.*, vol. 20, no. 3, pp. 1173–1185, Mar. 2021.

[16] A. M. Bedewy, Y. Sun, and N. B. Shroff, "Minimizing the age of information through queues," *IEEE Trans. Inf. Theory*, vol. 65, no. 8, pp. 5215–5232, Aug. 2019.

[17] C.-F. Liu and M. Bennis, "Taming the tail of maximal information age in wireless industrial networks," *IEEE Commun. Lett.*, vol. 23, no. 12, pp. 2442–2446, Dec. 2019.

[18] M. Chen, K. Wu, and L. Song, "A whittle index approach to minimizing age of multi-packet information in IoT network," *IEEE Access*, vol. 9, pp. 31467–31480, 2021.

[19] J. T. Gómez, K. Pitke, L. Stratmann, and F. Dressler, "Age of information in molecular communication channels," *Digit. Signal Process.*, vol. 124, May 2022, Art. no. 103108.

[20] M. A. Abd-Elmagid and H. S. Dhillon, "Average peak age-of-information minimization in UAV-assisted IoT networks," *IEEE Trans. Veh. Technol.*, vol. 68, no. 2, pp. 2003–2008, Feb. 2019.

[21] A. M. Bedewy, Y. Sun, R. Singh, and N. B. Shroff, "Optimizing information freshness using low-power status updates via sleep-wake scheduling," 2019, *arXiv:1910.00205*.

[22] D. Sinha and R. Roy, "Scheduling status update for optimizing age of information in the context of industrial cyber-physical system," *IEEE Access*, vol. 7, pp. 95677–95695, 2019.

[23] N. Hirosawa, H. Iimori, K. Ishibashi, and G. T. F. D. Abreu, "Minimizing age of information in energy harvesting wireless sensor networks," *IEEE Access*, vol. 8, pp. 219934–219945, 2020.
[24] H. Wei and N. Deng, "On the age of information in wireless networks using rateless codes," *IEEE Access*, vol. 8, pp. 173147–173157, 2020.
[25] A. Baiocchi and I. Turcanu, "Age of information of one-hop broadcast communications in a CSMA network," *IEEE Commun. Lett.*, vol. 25, no. 1, pp. 294–298, Jan. 2021.
[26] A. Maatouk, M. Assaad, and A. Ephremides, "On the age of information in a CSMA environment," *IEEE/ACM Trans. Netw.*, vol. 28, no. 2, pp. 818–831, Apr. 2020.
[27] M. Wang and Y. Dong, "Broadcast age of information in CSMA/CA based wireless networks," in *Proc. 15th Int. Wireless Commun. Mobile Comput. Conf. (IWCMC)*, Jun. 2019, pp. 1102–1107.
[28] M. Moltafet, M. Leinonen, and M. Codreanu, "Worst case age of information in wireless sensor networks: A multi-access channel," *IEEE Wireless Commun. Lett.*, vol. 9, no. 3, pp. 321–325, Mar. 2020.
[29] B. Zhou and W. Saad, "Performance analysis of age of information in ultra-dense Internet of Things (IoT) systems with noisy channels," *IEEE Trans. Wireless Commun.*, early access, Nov. 13, 2021, doi: 10.1109/TWC.2021.3122841.
[30] S. Kaul, M. Gruteser, V. Rai, and J. Kenney, "Minimizing age of information in vehicular networks," in *Proc. 8th Annu. IEEE Conf. Sensor, Mesh Ad Hoc Commun. Netw. (SECON)*, Jun. 2011, pp. 350–358.
[31] A. Baiocchi, I. Turcanu, N. Lyamin, K. Sjoöberg, and A. Vinel, "Age of Information in IEEE 802.11p," in *Proc. 17th IFIP/IEEE Int. Symp. Integr. Netw. Manage. (IM), ITAVT Workshop*, May 2021, pp. 1024–1031.
[32] D. Plöger, M. Segata, R. L. Cigno, and A. Timm-Giel, "Markov-modulated models to estimate the age of information in cooperative driving," in *Proc. IEEE Veh. Netw. Conf. (VNC)*, Dec. 2019, pp. 1–4.
[33] I. Turcanu, A. Baiocchi, N. Lyamin, and A. Vinel, "An age-of-information perspective on decentralized congestion control in vehicular networks," in *Proc. 19th Medit. Commun. Comput. Netw. Conf. (MedComNet)*, Jun. 2021, pp. 1–8.
[34] N. Lyamin, B. Bellalta, and A. Vinel, "Age-of-information-aware decentralized congestion control in VANETs," *IEEE Netw. Lett.*, vol. 2, no. 1, pp. 33–37, Mar. 2020.
[35] R. Molina-Masegosa, M. Sepulcre, J. Gozalvez, F. Berens, and V. Martinez, "Empirical models for the realistic generation of cooperative awareness messages in vehicular networks," *IEEE Trans. Veh. Technol.*, vol. 69, no. 5, pp. 5713–5717, May 2020.
[36] L. Kleinrock and F. Tobagi, "Packet switching in radio channels: Part I-carrier sense multiple-access modes and their throughput-delay characteristics," *IEEE Trans. Commun.*, vol. COM-23, no. 12, pp. 1400–1416, Dec. 1975.
[37] C. Bordenave, D. R. McDonald, and A. Proutière, "A particle system in interaction with a rapidly varying environment: Mean field limits and applications," *Netw. Heterogeneous Media*, vol. 5, no. 1, p. 31, 2010.
[38] A. Baiocchi, I. Turcanu, and A. Vinel, "To buffer or not to buffer: IEEE 802.11p/bd performance under different buffering strategies," in *Proc. 33rd Int. Teletraffic Congr. (ITC)*, Sep. 2021, pp. 1–9.
[39] M. F. Neuts, *Structured Stochastic Matrices of M/G/1 Type and Their Applications*. Boca Raton, FL, USA: CRC Press, 2021.
[40] A. Munari, "Modern random access: An age of information perspective on irregular repetition slotted Aloha," *IEEE Trans. Commun.*, vol. 69, no. 6, pp. 3572–3585, Jun. 2021.

ANDREA BAIOCCHI (Member, IEEE) received the Laurea degree in electronics engineering and the Ph.D. degree in information and communications engineering from the Sapienza University of Rome, in 1987 and 1992, respectively.

Since January 2005, he has been a Full Professor with the Department of Information Engineering, Electronics and Telecommunications, Sapienza University of Rome. He has published more than 160 papers on international journals and conference proceedings. He is the author of the book *Network Traffic Engineering: Stochastic models and Applications* (Wiley, 2020). His current research interests include massive multiple access, vehicular networking, congestion control for high bandwidth-delay product networks, and traffic monitoring and analysis. His research activities have been carried out also in the framework of many national (CNR, MIUR, and POR) and international (European Union and ESA) projects, also taking coordination and responsibility roles. He has participated to the technical program committees of more than 70 international conferences. He served in the editorial board of the telecommunications technical journal published by Telecom Italia (currently TIM) for ten years. He is currently an Associate Editor of *Vehicular Communications* (Elsevier) journal.

ION TURCANU (Member, IEEE) received the B.Sc. and M.Sc. degrees in computer science engineering and the Ph.D. degree in information and communications technologies from the Sapienza University of Rome, in 2011, 2014, and 2018, respectively. He is currently a Research and Technology Associate at the Luxembourg Institute of Science and Technology (LIST). Previously, he was a Postdoctoral Researcher at the Interdisciplinary Centre for Security, Reliability and Trust (SnT), University of Luxembourg. His research interests include next-generation cellular networks, multi-technology vehicular networks, wireless and mobile networks, and intelligent transportation systems.

ALEXEY VINEL (Senior Member, IEEE) received the Ph.D. degrees from the Institute for Information Transmission Problems, Moscow, Russia, in 2007, and from the Tampere University of Technology, Tampere, Finland, in 2013. He was a Professor II at the Western Norway University of Applied Sciences, Bergen, Norway, from 2018 to 2021. He has been a Professor with the School of Information Technology, Halmstad University, Halmstad, Sweden, since 2015 (part-time since 2022). He is currently a Professor at the Chair of Reliable Distributed Systems, University of Passau, Passau, Germany, since 2022, where he is heading the Chair of Reliable Distributed Systems. His research interests include wireless communications, vehicular networking, and cooperative autonomous driving.